Thesis for the degree of Licentiate of Engineering

Power Extraction in Military Aircraft

Performance of Low Bypass Ratio Mixed Flow Turbofan Engines with Large Power Extraction

Daniel Rosell

Department of Mechanics and Maritime Sciences
Division of Fluid Dynamics
CHALMERS UNIVERSITY OF TECHNOLOGY
Göteborg, Sweden 2023

Power Extraction in Military Aircraft
Performance of Low Bypass Ratio Mixed Flow Turbofan Engines with Large Power Extraction
Daniel Rosell

Licentiatavhandlingar vid Chalmers tekniska högskola
Technical report No. 2023:02

Department of Mechanics and Maritime Sciences
Division of Fluid Dynamics
Chalmers University of Technology
SE–412 96 Göteborg, Sweden
Telephone + 46 (0) 31 – 772 1000

Typeset by the author using LaTeX.

Printed by Chalmers Reproservice
Göteborg, Sweden 2023

To my family

Abstract

Military aircraft require more and more power. Pneumatic and hydraulic systems are being replaced by electrical equipment and new, power consuming equipment is introduced in the aircraft. Increased power extraction brings new challenges for the aircraft jet engine, both in terms of operability and with regards to engine performance.

This thesis describes how the engine performance of a conventional low bypass ratio mixed flow turbofan engine is affected by power extraction from the high-pressure shaft, the low-pressure shaft or a combination of the two.

A twin-spool low bypass ratio mixed flow turbofan engine has been developed in a Chalmers in-house tool to evaluate engine performance in different parts of the flight envelope. In order to evaluate the impact of aircraft/engine interaction on flight performance, an aircraft performance tool has been developed as well.

A turbine inlet gas temperature increase is required when power is extracted from the HP or LP shaft. This temperature increase is more considerable if power is extracted from the high-pressure shaft, increasing specific thrust and specific fuel consumption. When the engine is running close to, or at the maximum turbine inlet temperature limit, power extraction will have a detrimental impact on the engine performance, whether power is extracted from the high-pressure shaft or the low-pressure shaft, but the thrust reduction will be more substantial if power is extracted from the high-pressure shaft. When the engine is running close to or at the maximum overall pressure ratio limit, the thrust reduction due to high-pressure shaft power extraction is more moderate compared to the low-pressure shaft power extraction case, provided that the required temperature increase is acceptable from an engine operability perspective.

Keywords: Fighter aircraft performance, engine performance, low bypass ratio, mixed flow, turbofan engine, power extraction

Acknowledgments

I would like to thank my academic supervisor, Professor Tomas Grönstedt for his support, suggestions and turbofan engine model development. I also would like to thank my colleagues at Saab Aeronautics and particularly Michael Säterskog, Sebastian Arvidson, Hans Kling and Hans-Peter Magnusson for valuable technical and practical support throughout the project and for giving me the opportunity to become an industrial Ph.D student. Further, I would like to acknowledge the work of Pedro David Bravo-Mosquera who has provided a conceptual aircraft design for the engine performance study.

This work has been funded by the Swedish Governmental Agency for Innovation Systems (VINNOVA), the Swedish Defense Materiel Administration (FMV) and the Swedish Armed Forces within the International Aviation Research Programme (IFFP diary number 2020-00690) and Saab Aeronautics.

Daniel Rosell
Linköping, March 2023

List of Publications

This thesis is based on the following appended papers:

Paper 1. Daniel Rosell and Tomas Grönstedt. *Design Considerations of Low Bypass Ratio Mixed Flow Turbofan Engines with Large Power Extraction.* Fluids 2022, 7(1), 21.

Paper 2. Daniel Rosell, Tomas Grönstedt, Pedro David Bravo-Mosquera, Fernando Martini Catalano. *Low BPR Turbofan Performance with Power Extraction.* 33rd Congress of the International Council of the Aeronautical Sciences, Stockholm, Sweden, 2022.

Other relevant publications co-authored by Daniel Rosell:

Marcelo Assato, Ali Altar Incer, Lucilene Moraes, Jesuino Takachi Tomita, Cleverson Binghenti, Pedro Bravo-Mosquera, **Daniel Rosell**, Tomas Grönstedt. *Performance Benefits of a Fan on Blade - FLADE - For a Variable Cycle Engine.* 33rd Congress of the International Council of the Aeronautical Sciences, Stockholm, Sweden, 2022.

Nomenclature

Abbreviations

A	–	area
A/B	–	afterburner
AC	–	alternating current
ACE	–	adaptive cycle engine
ACM	–	air cycle machine
AMAD	–	airframe mounted accessory drive
AR	–	aspect ratio
A_c	–	capture area
APU	–	accessory power unit
BPR	–	bypass ratio
C_D	–	drag coefficient
C_{D_0}	–	zero-lift drag coefficient
C_{fe}	–	equivalent skin friction coefficient
C_L	–	lift coefficient
C_{L_α}	–	lift curve slope
$C_{L_{design}}$	–	design lift coefficient
C_{TO}	–	corrected power take-off
c_p	–	specific heat at constant pressure
D	–	drag
DC	–	direct current
D_s	–	spillage drag
E	–	energy
E_s	–	specific energy
E_{wd}	–	wave-drag efficiency factor
EHP	–	electrical hydraulic pump
EMAD	–	engine mounted accessory drive
F	–	force
FADEC	–	full authority digital engine control
F_N	–	net thrust
f_s	–	fuel specific energy
FPR	–	fan pressure ratio
GESTPAN	–	general stationary and transient propulsion analysis

HP – high-pressure
HPC – high-pressure compressor
HPCPR – high-pressure compressor pressure ratio
HPT – high-pressure turbine
h – enthalpy
h – height
K – drag due to lift factor
K_{100} – drag due to lift factor with 100 % leading-edge suction
K_0 – drag due to lift factor with 0 % leading-edge suction
L – lift
L/D – lift-to-drag ratio
LP – low-pressure
LPC – low-pressure compressor
LPT – low-pressure turbine
M – Mach number
M_{DD} – drag-divergent Mach number
MFR – mass flow ratio
MHP – main hydraulic pump
MIL – military power (maximum non-augmented power)
MAX – maximum augmented power (A/B in operation)
$\dot{m}$ – mass flow
n_e – number of engines
OPR – overall pressure ratio
P – power
P_s – specific power
P_{TO} – absolute power take-off
PTS – power transmission shaft
p – pressure
p_0 – stagnation pressure
q – dynamic pressure
R – range
R_s – specific range
S – leading-edge suction parameter
SFC – specific fuel consumption
S_{ref} – wing reference area
S_{wet} – aircraft wetted area
SLS – sea level static

T	–	temperature
T	–	installed thrust
T_0	–	stagnation temperature
TB	–	thermal battery
TRU	–	transformer rectifying unit
T/W	–	thrust-to-weight ratio
$(T/W)_{TO}$	–	take-off thrust-to-weight ratio
V	–	velocity
V_G	–	ground speed
V_∞	–	true air speed
VCE	–	variable cycle engine
W	–	weight
W_e	–	empty weight
W_p	–	payload weight
W_{TO}	–	take-off weight
W/S	–	wing loading
$(W/S)_{TO}$	–	take-off wing loading

Greek

α_{shock}	–	ratio of intake supersonic loss to normal shock loss
α_{spill}	–	spillage drag to pre-entry drag ratio
β	–	aircraft weight fraction relative to takeoff weight
β_f	–	fuel schedule factor, off-design fuel flow relative to the design point fuel flow
β_{fan}	–	operating line offset in fan map
β_{HPC}	–	operating line offset in HPC map
γ	–	aircraft climb angle
γ	–	ratio of specific heats
δ	–	non-dimensional pressure (p/p_{SLS})
δ_0	–	non-dimensional stagnation pressure (p_0/p_{SLS})
ϵ	–	thrust inclination angle compared to free stream
θ	–	non-dimensional temperature (T/T_{SLS})
θ_0	–	non-dimensional stagnation temperature (T_0/T_{SLS})
θ_{0break}	–	theta break, θ_0 where the engine is operating at OPR_{max} and T_{4max}
Λ	–	sweep
Λ_{LE}	–	leading-edge sweep
ρ	–	density

Subscripts

0	–	stagnation
1	–	air intake
2	–	fan inlet
3	–	high-pressure compressor delivery
4	–	high-pressure turbine inlet
5	–	low-pressure turbine exit
6	–	front face of afterburner
7	–	nozzle inlet
8	–	nozzle throat
9	–	nozzle exit
∞	–	free-stream
a	–	air
c	–	conditions at entry (of intake)
max	–	maximum value (T_4, OPR)
pre	–	pre-entry
x	–	velocity direction
z	–	direction perpendicular to the velocity direction

Contents

Part I

Introductory chapters

Chapter 1

Introduction

1.1 Background

Power is required for different equipment in air vehicles. Traditional power consumers are pumps and systems used for hydraulic, pneumatic and control [1, 2]. Control systems have evolved from mechanical systems to full authority electrical control systems such as fly-by-wire for flight control and full authority digital engine control (FADEC) for engine control [3].

Figure 1.1: Gripen fighter during take-off.

Power is usually extracted by a generator, via an engine mounted accessory drive, EMAD [4]. This accessory drive adds to the aircraft cross-sectional area, but if the generator could be mounted directly to the shaft as described in [5, 6], the engine and aircraft cross-sectional area could be reduced, which is desirable for military aircraft, with supersonic capability [7–9].

A layout of a typical power flow system in an aircraft is shown in Figure 1.2 [10, 11]. Auxiliary Power Units (APUs) can be used in arrangements with accessory drive

gearboxes to power hydraulic pumps and electrical generators for ground checkout of the hydraulic and electrical power systems, to provide shaft power for engine starting and as an in-flight emergency power source [12]. APUs can also be used to provide compressed air for purposes such as thermal anti-icing and defogging [12].

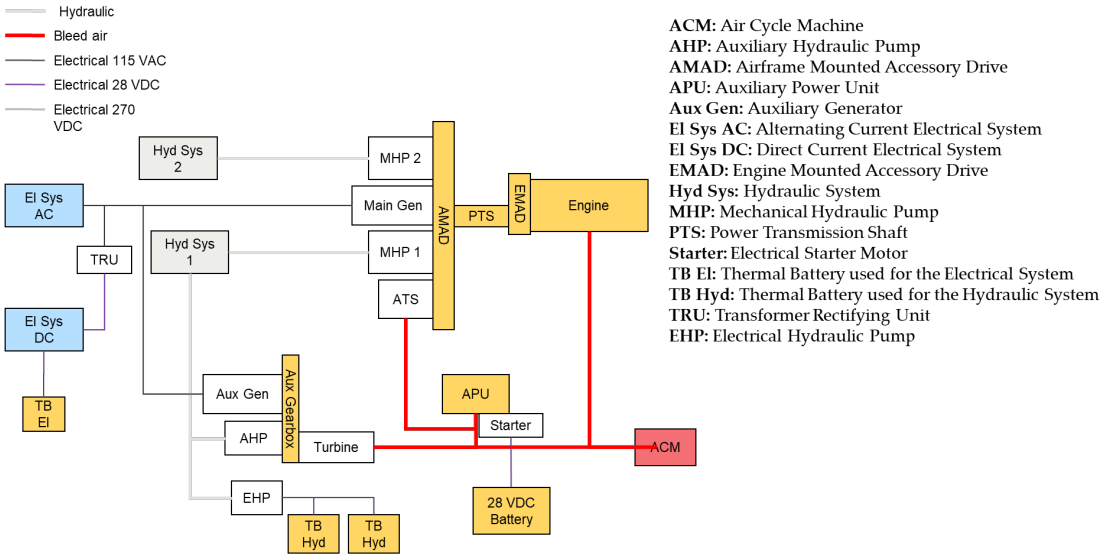

Figure 1.2: A typical layout of power flow between systems in an aircraft. Based on figures in [10, 11].

The amount of power consumed is continuously increasing [13]. Introduction of new, power consuming electrical equipment such as advanced radars and mission systems [14] and the transition of hydraulic systems to electric machinery [3, 15–18] contributes to an increased need for electrical power. An overview of a vehicle system, with some power consumers is shown in Figure 1.3 [19].

In the late 1980's and early 90's a development started, where central hydraulic equipment in military aircraft was replaced by electric systems [3, 14, 20]. This development was primarily driven by goals to improve reliability, maintainability and supportability, but also with the aim to reduce volume and weight of the concerned systems [20, 21].

Increasing the amount of power extracted from the fighter aircraft jet engine will place new demands on the engine, both from a performance and from an operability point of view, but the challenges will not be limited to the engine. Avionics, electromechanical flight control actuators, engine accessories, and weapon and mission systems not only consume more power, they also generate excessive heat, which must be handled by the aircraft [22, 23]. Moreover, an increased heat load raises the power that is required by coolant pump(s), which in turn increases the required power and the heat generated by the propulsion system [24]. All in all, this contributes to completely new demands being placed on the aircraft's cooling system [14].

The impact of power extraction on turbofan engines with high bypass ratio have previously been investigated [25–29]. For military applications, investigations on engine power extraction have been performed for alternative cycles [30, 31]. A typical

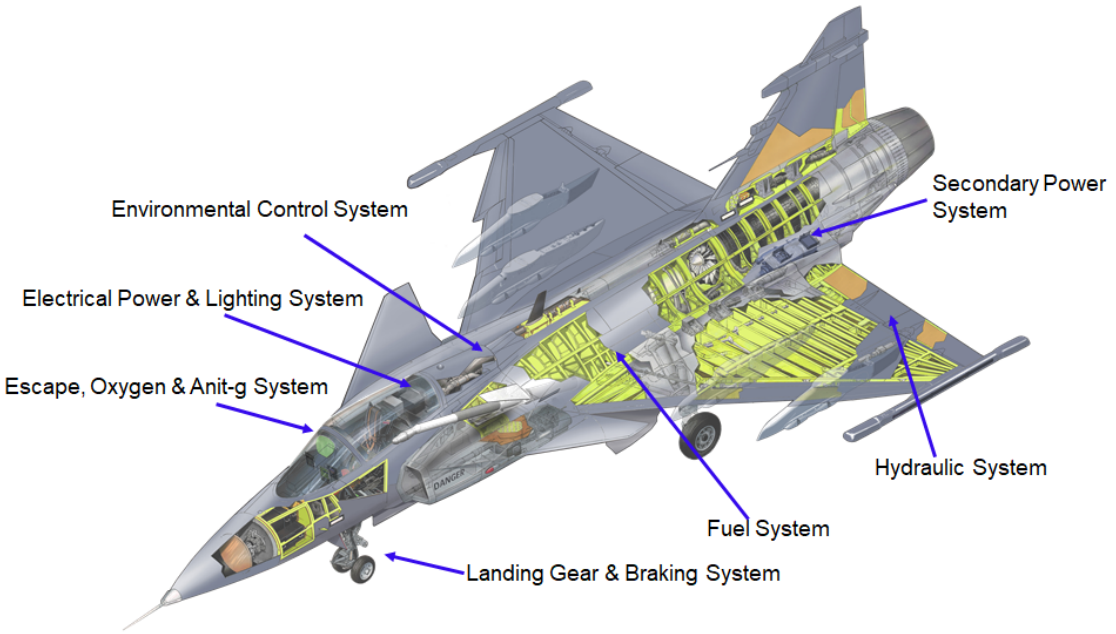

Figure 1.3: An overview of the Gripen aircraft vehicle systems [19].

fighter aircraft engine is a twin-spool low bypass ratio mixed flow turbofan engine, this engine type is by far the most common engine of today's fighter aircraft. Paying attention to the effect of power extraction from this type of engine is well justified by the fact that power consumption has increased significantly in military aircraft over the past few decades [22].

In twin-spool engines, power can be extracted from either the high-pressure (HP) shaft or the low-pressure (LP) shaft. Previous investigations with high bypass ratio engines have indicated that performance benefits [25–27] and operability benefits [25–28] can be achieved if power extraction can be distributed between the low-pressure and high-pressure shaft. It will be shown that similar benefits can be achieved for a low bypass ratio mixed flow turbofan engine if power can be distributed between the LP shaft and the HP shaft, depending on the aircraft mission phase concerned, but the additional weight added by such solutions must be considered.

This thesis summarizes findings from a joint project with Saab Aeronautics, Chalmers university of technology, University of São Paulo and GKN Aerospace.

The thesis is divided into two main parts. The first part gives an introduction to the research field, describes work that has been carried out and results achieved. The second part consists of appended research papers.

1.2 Method

An aircraft mission has been developed and a conceptual aircraft design has been carried out by University of São Paulo, using an in-house tool, as described in section 2.1. The aircraft thrust requirements have been used as design requirements for the engine design work, illustrated in chapter 3.

A low bypass ratio mixed flow turbofan engine was modeled in the Chalmers in-house tool GESTPAN [32], the methodology is described in section 3.1, and thermodynamic cycle parameters have been decided, as described in section 3.3, to meet the engine thrust requirement given in section 2.1.

To evaluate engine performance in different parts of the aircraft flight envelope, engine simulations are carried out as off-design simulations. The investigation is based on a large number of off-design simulations carried out, not only for the aircraft mission requirement points, but also at various part power levels, at military power and maximum augmented power throughout the aircraft operating flight envelope. Handling such a huge amount of data, requires a tool for data processing. A tool has been developed in MATLAB and is used to

- specify and store design parameters such as FPR, HPCPR, BPR and T_4
- specify and store input conditions such as altitudes, Mach numbers, engine power levels, constraints, bleed flows and amounts of power extraction for the off design simulations
- generate and store input files to GESTPAN in specified folders
- initiate the GESTPAN simulations
- store the GESTPAN simulation files in specified folders
- import, structure and store data from the GESTPAN simulation and performance files in MATLAB
- quickly modify the design point and simulate the off-design points, corresponding to the aircraft mission thrust requirement points in order to evaluate different thermodynamic cycle designs

In addition to this, the developed tool contains about a hundred functions for processing of engine input and simulation data.

The thermodynamic cycle of the design point is evaluated against the thrust requirements in the off-design simulations, but also from a more general aircraft performance perspective throughout the flight envelope. To be able to perform interactive aircraft/engine studies, an aircraft performance model has been developed. Characteristics of this aircraft performance model, developed to produce realistic estimates of aircraft drag and thrust requirements for typical fighter aircraft maneuvers, is reported in section 2.2.

To study the impact of power extraction from the HP shaft, the LP shaft or a combination of the two, four specific cases have been studied:

1. Baseline - no power extraction
2. HP shaft power extraction 900 kW
3. LP shaft power extraction 900 kW
4. Combined shaft power extraction 450 kW LP shaft and 450 kW HP shaft

To clearly illustrate the impact of power extraction on engine performance, 900 kW was chosen as a high, yet reasonable amount of power extraction for jet engines in the selected thrust class. Nevertheless, such large amounts of power extraction will present significant challenges to the turbofan engine, particularly at high altitude / low speed and part power cases [33]. To reflect this varying impact with ambient conditions, corrected power take-off, C_{TO}, defined in Equation (1.1), is sometimes used instead of absolute power take-off, P_{TO} [34]. In Equation (1.1), $h_0 = c_p T_0$. However, while the impact on engine performance varies with ambient conditions, the power consumed by aircraft equipment does not change in the same way, hence a constant amount of power extraction is assumed.

$$C_{TO} = \frac{P_{TO}}{\dot{m}_a h_0} \tag{1.1}$$

In [34] a power requirement of 300 kW for an air-to-air fighter is specified. Traditional power consumption has been in the order of 100 kW according to [30]. A power extraction requirement of 300 kW for a 50 kN civil aircraft engine is specified in [35]. This can be compared to a cruise case for the fighter aircraft, where the required thrust is around 10 kN per engine.

1.3 Limitations

The work performed and presented in this thesis is primarily from an engine performance perspective and aims to illustrate the principal engine behavior due to power extraction from the HP shaft, the LP shaft or a combination of the two. The engine performance potential of LP and HP shaft power extraction described may be limited due to operability requirements such as surge margins and overspeed limitations. For instance, large amounts of HP power extraction at high altitude/low speed will reduce compressor surge margins and the required aerodynamic HPC overspeed margin required to maintain thrust when power is extracted from the LP shaft may have an impact on sizing of the HPC, i.e. the compressor might have to be aerodynamically designed for a higher pressure ratio and higher corrected mass flow [9]. Operability limitations are often related to engine transients, which are not considered here.

There may be practical advantages to one or the other solution that are not considered further here. Traditionally, power extraction from the HP shaft has often been preferred due to its higher speed and its limited speed range as well as engine starting requirements [6]. Higher speed and limited speed range reduce the size of the electrical machine [27].

The engine control is limited by either the maximum OPR limit, OPR_{max} or the maximum turbine inlet temperature limit, T_{4max} which is a simplification, as described in section 3.4. On the outskirts of the engine operating envelope, other engine limitations may limit engine performance further. Aircraft afterbody drag is neglected, when estimating installed engine thrust, T.

The aircraft performance model, described in section 2.2 is developed to produce realistic thrust and drag requirements for a typical fighter aircraft, not to reproduce

the aerodynamics of an existing fighter aircraft or provide accurate aerodynamic predictions of a certain conceptual aircraft design. This approach is deemed sufficient for the studies of interest at this level.

Chapter 2

Aircraft conceptual design

Defining threats, targets and future scenarios is part of the process when determining the requirements of a fighter aircraft [36]. A conceptual fighter aircraft design has been carried out by University of São Paulo to achieve a balanced aircraft design, in which characteristics such as weight, aerodynamics configuration, aircraft size and an initial aircraft performance estimation has been produced. A brief summary of the conceptual aircraft design is given in [36]. Selected aspects of this conceptual design is reflected in section 2.1 below. The requirements of this conceptual design is the basis for the engine design, described in chapter 3.

As the design process continues, a need to evaluate aircraft performance from a more general perspective emerges and the initial aircraft performance estimation must be updated with updated engine performance data. To be able to perform interactive aircraft/engine studies and evaluate power extraction impact on flight performance for different flight maneuvers, an aircraft performance model has been developed. The characteristics of the performance model is given in section 2.2.

2.1 Aircraft mission and conceptual design

The design requirements for the fighter aircraft design has been worked out to achieve close-in-combat and beyond visual range combat capability to achieve superiority in the air-to-air role [36]. Other requirements are short take-off and landing distances, high sortie rates and abilities for air-to-surface missions [37]. The continuous strive for increased survivability of fighter aircraft [38] raises the need for reduced radar cross-section to avoid detection by enemy radar and aircraft ruggedness to be able to return to base even after some damage has been inflicted. Other objectives, which guided the aircraft design are listed below [36]:

- High thrust-to-weight ratio (T/W) to improve low altitude maneuverability and to enable rapid ingress and egress from the combat area.
- High weapons load capacity to be able to engage a large number of targets.
- High supersonic speed for quick escape dash and evasion [34, 39–41].
- High range and endurance on target to be able to support ground troops for an extended period of time.

A typical fighter design mission profile, illustrated by Figure 2.1, has been defined with the following phases included:

1. Warm-up and take-off
2. Acceleration and climb
3. Subsonic cruise
4. Payload drop
5. Combat
6. Escape dash
7. Subsonic cruise
8. Fuel reserves
9. Descend to land

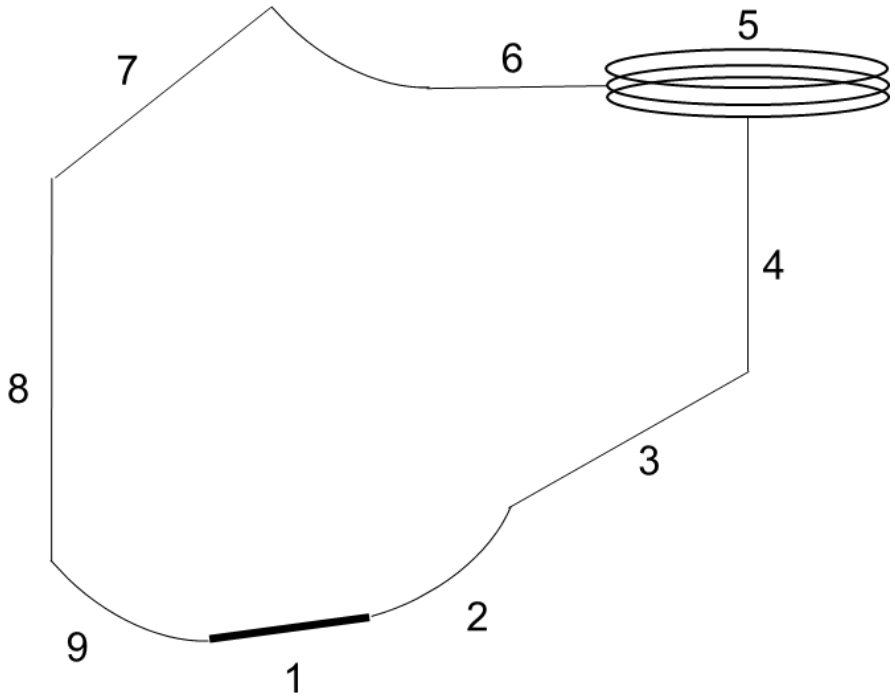

Figure 2.1: Design mission profile [34, 36].

Operational requirements, such as payload weight, flight endurance and flight velocities, were defined based on the design mission profile. A tool, previously used for other fighter aircraft configurations [42], developed at University of São Paulo, was used for presizing and performance requirement calculations. A double engine configuration was chosen and preliminary characteristics of the aircraft is presented in Table 2.1. Thrust requirements per engine in key parts of fighter mission are specified in Table 2.2, for the phases illustrated in Figure 2.1. An overview of the conceptual fighter aircraft is provided in Figure 2.2.

Table 2.1: Aircraft characteristics.

Max take-off weight	W_{TO}	21,920 kg
Empty weight	W_e	12,620 kg
Payload weight	W_p	4500 kg
Take-off wing loading	$(W/S)_{TO}$	3360 Pa
Range	R	1500 nm
Number of engines	n_e	2

Table 2.2: Thrust requirements per engine.

No.	**Mission phase**	**Description**	**A/B**	**Req. thrust**	**Altitude**	**M**
1	1	Warm-up	no	66.0 kN	610 m	0.0
2	1	Runway acceleration	yes	110.7 kN	610 m	0.1
3	1	Runway acceleration	yes	112.9 kN	610 m	0.18
4	2	Flight acceleration	yes	127.3 kN	610 m	0.44
5	2	Climb and acceleration	yes	127.8 kN	2743 m	0.775
6	2	Climb and acceleration	yes	78.9 kN	7010 m	0.875
7	3	Subsonic cruise	no	12.4 kN	9144 m	0.9
8	5	Sustained turn	yes	100.6 kN	9144 m	1.6
9	5	Sustained turn	yes	53.2 kN	9144 m	0.9
10	6	Escape dash	yes	113.9 kN	9144 m	2.0

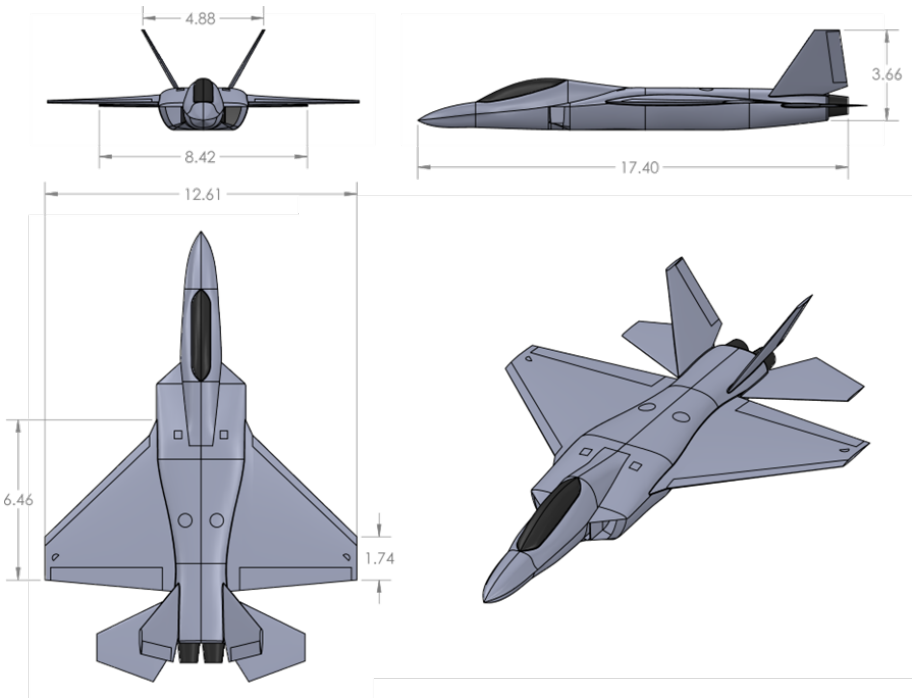

Figure 2.2: Four views of the fighter aircraft concept, from [36].

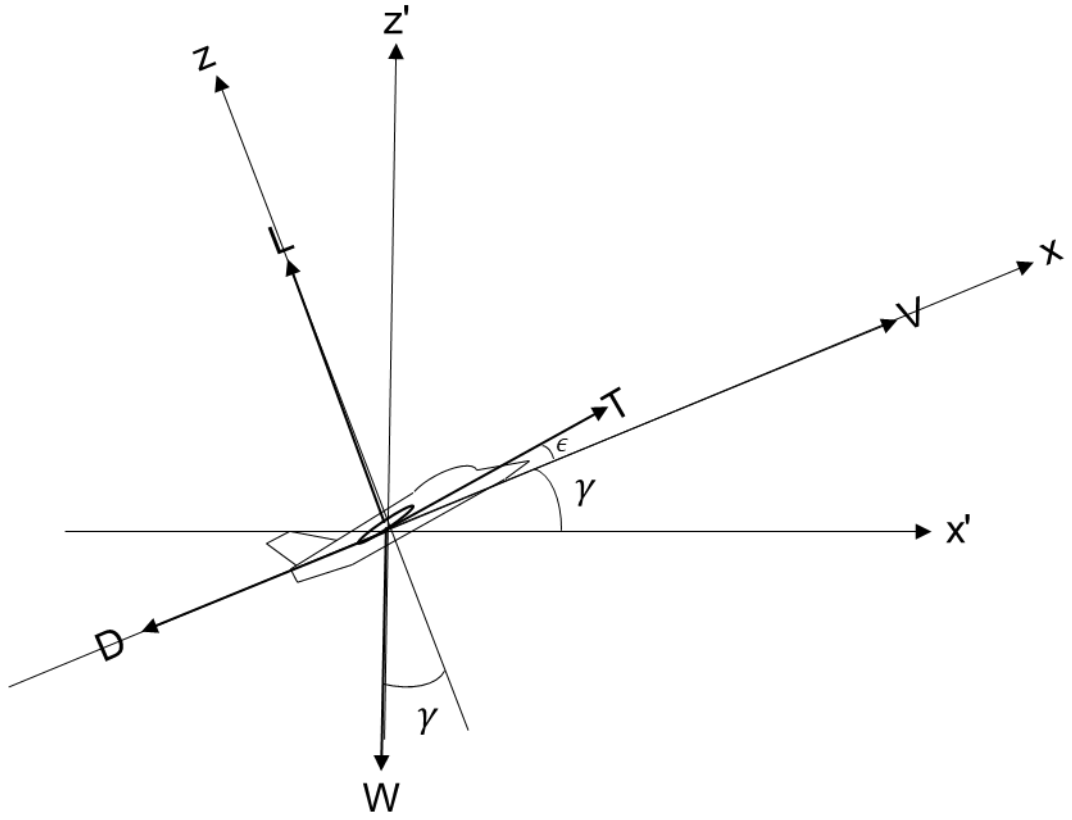

Figure 2.3: Forces affecting the aircraft.

2.2 Aircraft performance modeling

The mission thrust requirements presented in Table 2.2 are used to identify an appropriate engine design to meet the basic constraints of the fighter aircraft, as described in chapter 3. When improved engine performance data becomes available, the initial aircraft performance estimates must be updated and aircraft performance can be evaluated from a more general perspective.

An aircraft performance model has been developed to produce realistic performance estimations in different flight cases, based on methods described in [43–46], to perform interactive aircraft/engine performance studies and more accurate mission simulations.

The basic equations (2.1) and (2.2), illustrated in Figure 2.3, from Newton's second law of motions, are used to calculate forces in the velocity direction and in the direction perpendicular to the velocity direction of a wind axis system.

$$\sum F_x = T\cos\epsilon - D - W\sin\gamma \tag{2.1}$$

$$\sum F_z = T\sin\epsilon + L - W\cos\gamma \tag{2.2}$$

As long as the thrust inclination angle, ϵ is rather small, i.e. $\cos\epsilon \approx 1$ and $\sin\epsilon \approx 0$, its impact may be neglected. This quite common simplification is used for

all aircraft performance calculations. V is the true airspeed of the aircraft, often referred to as V_∞. Wind is disregarded, hence $V = V_\infty = V_G$ [44].

Specific energy E_s, given by Equation (2.3) and specific excess power P_s, given by Equation (2.4) are used to calculate aircraft performance in maneuvers such as climbs and accelerations [43, 44]. Fuel specific energy, reflected by Equation (2.5), is used to estimate the most fuel efficient flight path in different maneuvers and specific range R_s, which is used to estimate cruise performance, is calculated using Equation (2.6) [43][1].

$$E_s = h + \frac{V^2}{2g} \tag{2.3}$$

$$P_s = \frac{V(T-D)}{W} = \frac{dh}{dt} + \frac{V}{g}\frac{dV}{dt} \tag{2.4}$$

$$f_s = \frac{dE_s}{dW_f} = \frac{dE_s/dt}{dW_f/dt} = \frac{P_s}{SFC \times T} \tag{2.5}$$

$$R_s = \frac{dR}{dW} = \frac{V}{-SFC \times T} \tag{2.6}$$

The aircraft drag coefficient is calculated, using Equation (2.7) [43–45], where drag (D) and lift (L) are given by Equation (2.8), (2.9) and (2.10).

$$C_D = C_{D_0} + KC_L^2 \tag{2.7}$$

$$D = qS_{ref}C_D \tag{2.8}$$

$$L = qS_{ref}C_L \tag{2.9}$$

$$q = \frac{1}{2}\rho V^2 \tag{2.10}$$

[1]Please note that the definition of SFC in Equation (2.6) and (2.5) is $SFC \equiv \frac{dW_f/dt}{T}[\frac{N/s}{N}]$. SFC can also be defined as $SFC \equiv \frac{dm_f/dt}{T}[\frac{kg/s}{N}]$ or $[\frac{mg/s}{N}]$.

2.2.1 Parasite drag

Subsonic parasite drag may be estimated by Equation (2.11) [43, 45, 47, 48], where C_{fe} is the equivalent skin friction coefficient. A typical value of C_{fe} for an air force fighter aircraft is 0.0035 [43, 47, 48], but varies from one aircraft to the other, depending on factors such as relative wing size, fuselage shape and aerodynamic cleanness [48]. Subsonic parasite drag characteristics of ten different jet fighter aircraft are evaluated in [48], where the equivalent skin friction drag varies from 0.0032 to 0.0052.

$$C_{D_0} = C_{fe}\frac{S_{wet}}{S_{ref}} \tag{2.11}$$

Supersonic zero lift drag consists of skin friction drag and wave drag. The skin friction share is assumed to be two-thirds of the subsonic zero lift drag [45, 47, 48]. Wave drag is estimated by Equation (2.12), using a method proposed in [43], where the leading-edge sweep Λ_{LE} is given in degrees. The $(\frac{D}{q})_{Sears-Haack}$ term in Equation (2.12) corresponds to the drag of an ideal Sears-Haack body [49] given by Equation (2.13).

$$\left(\frac{D}{q}\right)_{wave} = E_{wd}\left[1 - 0.2(M-1.2)^{0.57}\left(1 - \frac{\pi\Lambda_{LE}{}^{0.77}}{100}\right)\right]\left(\frac{D}{q}\right)_{Sears-Haack} \tag{2.12}$$

$$\left(\frac{D}{q}\right)_{Sears-Haack} = \frac{9\pi}{2}\left(\frac{A_{max}}{l}\right) \tag{2.13}$$

Transonic parasite drag is calculated following procedures proposed in [43, 47].

2.2.2 Lift induced drag

The subsonic drag due to lift factor is estimated, using the leading-edge suction method [42, 43, 45, 47, 48, 50], given by Equation (2.14), (2.15) and (2.16).

$$K = SK_{100} + (1 - S)K_0 \tag{2.14}$$

$$K_{100} = \frac{1}{\pi AR} \tag{2.15}$$

$$K_0 = \frac{1}{C_{L_\alpha}} \tag{2.16}$$

The leading-edge suction parameter S is calculated as a function of C_L and $C_{L_{design}}$, see Equation (2.17). A C_L design value of 0.18 was used for the aircraft performance simulations presented in section 4.2. The leading-edge suction parameter variation with C_L is shown in Figure 2.4.

$$S = f(C_L, C_{L_{design}}) \tag{2.17}$$

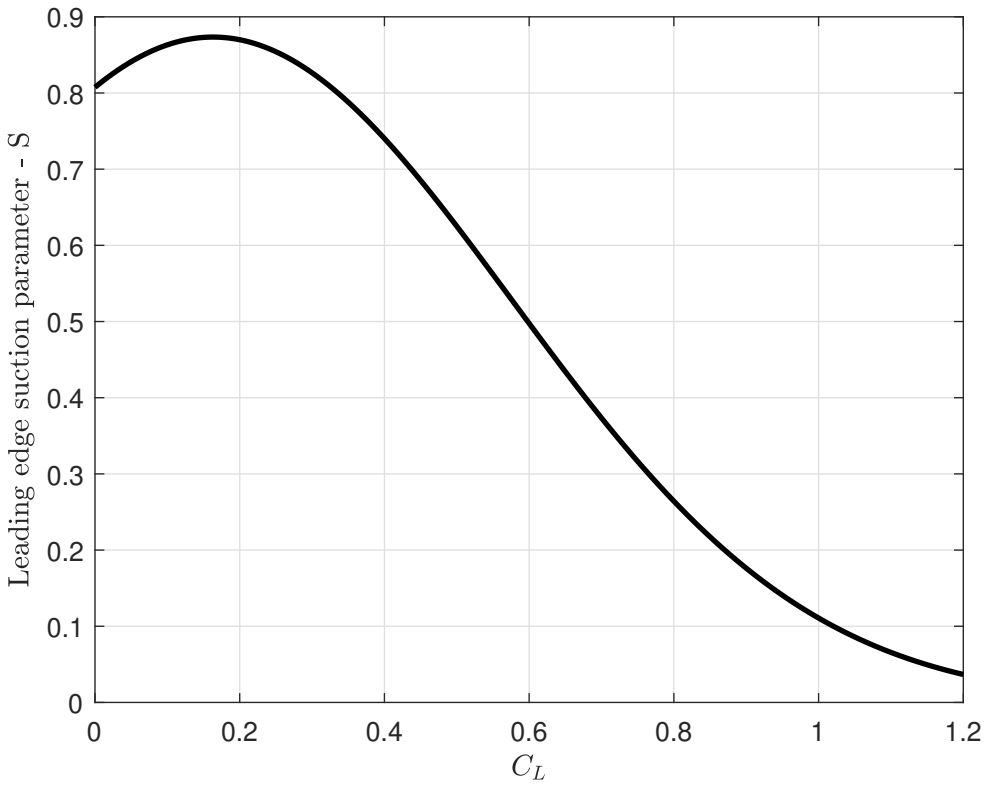

Figure 2.4: Leading-edge suction with $C_{L_{design}} = 0.18$.

In the transonic region, starting at the drag divergence Mach number M_{DD}, the leading-edge suction is gradually decreased to zero with increasing Mach number up to the point where the wing leading-edge becomes supersonic.

Chapter 3

Engine design

To meet the requirements of section 2.1 and Table 2.2, a low bypass ratio mixed flow turbofan engine model has been developed and an engine design has been proposed. Section 3.1 describes the engine modeling procedure, section 3.2 depicts how aircraft installation effects are estimated, section 3.3 motivates engine sizing and design point selection and section 3.4 handles limitations and constraints of the off-design calculations.

3.1 Engine performance modeling

A twin-spool low bypass ratio mixed flow turbofan engine has been modeled in the tool GESTPAN (GEneral Stationary and Transient Propulsion ANalysis) [32]. GESTPAN uses a traditional approach for gas turbine implementation, with two different modes of simulation:

1. Design mode
2. Off-design mode

The design mode allows the user to specify parameters from the preliminary design phase [32]. For the low bypass ratio mixed flow turbofan engine studied, these design parameter choices are described more closely in section 3.3.

The interaction of the engine modules are governed by compatibility requirements [51]:

- Compatibility of work
- Compatibility of flow
- Compatibility of rotational speed

Differential algebraic equations emerge when algebraic constraints are imposed on the states of a physical system that is modeled with differential equations [52]. An important aspect in the simulation and control of dynamic systems is that conservation laws, i.e. conservation of mass and momentum, are preserved. Such algebraic relations pose constraints on the solution of the differential equations [52].

A special class of differential algebraic equations are semi-explicit differential algebraic equations, which are ordinary differential equations with constraints [53, 54]. GESTPAN uses graph theory to assemble a set of equations automatically, generally represented by a system of semi-explicit non-linear differential algebraic equations [32, 55] given by Equation (3.1).

$$\begin{aligned} \mathbf{x'} &= f(\mathbf{x}, \mathbf{z}) \\ \mathbf{0} &= g(\mathbf{x}, \mathbf{z}) \end{aligned} \tag{3.1}$$

The system of semi-explicit non-linear algebraic equations represented by Equation (3.1) appear frequently in applications. It arises in the modeling of electrical networks, constrained mechanical systems, vehicle dynamics, in the solutions of the equations of fluid flow [56, 57] and it is the most probable system of equations emerging when modeling an arbitrary gas turbine system [32, 55]. In Equation (3.1), the x variables are referred to as differential variables and the z variables as algebraic variables [55]. When steady state operating conditions are considered, **x'** in Equation (3.1) becomes a zero vector (i.e. $x'_1 = x'_2 = ... = x'_n = 0$). A secant method with Broyden update for the Jacobian [58, 59] is used by the equation solver and is implemented in [60].

The turbofan engine model consists of the following modules:

- Intake
- Fan (LPC)
- Splitter
- High-pressure compressor (HPC)
- Combustor
- High-pressure turbine (HPT)
- Low-pressure turbine (LPT)
- Unifier (mixer)
- Afterburner (A/B)
- Nozzle

Detailed descriptions of the different modules are given in Appendix A in [32], with complementing information on intake implementation in section 3.2 below. An overview of the modeled engine is provided in Figure 3.1 with standardized station numbering, as specified in Table 3.1, according to [62].

The iteration variables and residuals used for the modeled low bypass ratio mixed flow turbofan engine are given in Table 3.2.

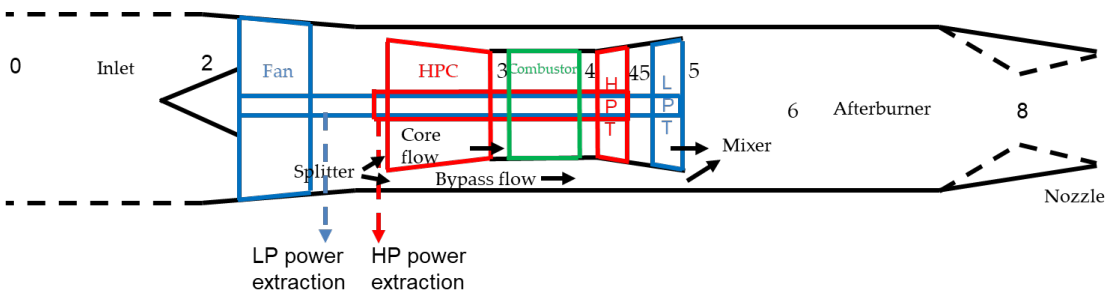

Figure 3.1: Overview of the modeled turbofan engine, based on figures in [36, 61].

Table 3.1: Engine station numbering.

Station	**Location**
0	Free stream
1	Air intake
2	Fan inlet
3	HPC delivery
4	HPT inlet
5	LPT exit
6	Front face of afterburner
7	Nozzle inlet
8	Nozzle throat
9	Nozzle exit

Table 3.2: Iteration variables and residuals of the GESTPAN calculations.

Iteration variables	**Residuals**
Inlet mass flow	Inlet flow compatibility
Fan map β_{fan}	Core flow compatibility
Fan rotation speed	Fan/LPT work compatibility
Bypass ratio	HPC/HPT work compatibility
HPC map β_{HPC}	HPT inlet flow compatibility
HPC rotation speed	LPT inlet flow compatibility
Fuel schedule factor β_f	Static pressure match in unifier
HPT outlet pressure	Afterburner flow compatibility
LPT outlet pressure	Engine control residual

3.2 Aircraft installation effects

The performance of a jet engine is affected when it is installed in an aircraft. In addition to the losses caused by power extraction, installation losses are inflicted due to bleed flow extraction to the airframe [63], pressure losses and spillage drag of the intake [64] and afterbody drag [34]. In the performed simulations, no bleed flow is extracted and afterbody drag is neglected. The impact on engine performance from these installation effects are usually rather small and varies with flight conditions and engine power level. To give an idea of the magnitude, a performance loss of approximately 2 to 3 percent at military and maximum augmented power per lb/s of bleed power extraction was reported for the F404 engine in [65] and losses due to afterbody drag are estimated to 3 percent in [42].

To estimate intake losses, a simplified intake model has been developed including estimates on intake pressure losses and spillage drag.

Modeled intake losses include:

- lip losses
- duct losses
- supersonic losses

Mass flow ratio (MFR), given by Equation (3.2), is essential for intake loss and spillage drag estimations. In Equation (3.2), A_∞ represents the area of the stream tube entering the engine, V_∞ is the free stream velocity and ρ_∞ is the air density. A_c is the inlet capture area. The mass flow entering the engine is given by Equation (3.3).

$$MFR = \frac{A_\infty}{A_c} = \frac{\dot{m}_a}{A_c V_\infty \rho_\infty} \tag{3.2}$$

$$\dot{m}_a = A_\infty V_\infty \rho_\infty \tag{3.3}$$

Lip losses

Lip losses are calculated as a function of mass flow ratio (MFR), see Equation (3.4), where the losses increase asymptotically towards the assumed maximum loss. MFR is given by Equation (3.2).

$$\left(\frac{\Delta p}{p_0}\right)_{lip} = f(MFR) \tag{3.4}$$

Duct losses

Duct losses are assumed to increase exponentially as a function of corrected mass flow, see Equation (3.5), where the maximum duct loss, used as input to Equation (3.5) depends on the duct area.

$$\left(\frac{\Delta p}{p_0}\right)_{duct} = f\left(\frac{\dot{m}\sqrt{T_0}}{p_0}\right) \tag{3.5}$$

Supersonic losses

Supersonic losses are highly related to shock losses and are calculated as a fraction of a normal shock loss, as shown in Equation (3.6). In Equation (3.6) p_{01} and p_{02} are stagnation pressures before and after a normal shock, represented by Equation (3.7) [1]. Intakes can be more or less well adapted for supersonic flight. A supersonic loss factor $\alpha_{shock} = 0.75$ has been used for the simulations presented in chapter 4.

$$\left(\frac{\Delta p}{p_0}\right)_{supersonic} = \alpha_{shock}\left(1 - \frac{p_{02}}{p_{01}}\right) \tag{3.6}$$

$$\left(\frac{p_{02}}{p_{01}}\right) = \left(\frac{(\gamma+1)M^2}{(\gamma-1)M^2+2}\right)^{\frac{\gamma}{\gamma-1}} \left(\frac{\gamma+1}{2\gamma M^2-(\gamma-1)}\right)^{\frac{1}{\gamma-1}} \tag{3.7}$$

Spillage drag

Spillage drag is estimated as a fraction of pre-entry drag as shown by Equation (3.8), where the pre-entry drag D_{pre} is calculated, using Equation (9.4) in [64] reproduced here as Equation (3.9), where the pre-entry drag coefficient, $C_{D_{pre}}$ is given by Equation (3.10) [64]. Some of the pre-entry drag, i.e. $(1 - \alpha_{spill})D_{pre}$ can be recovered when the flow is accelerated around the intake lips [64]. This recovered pre-entry drag, referred to as cowl thrust, and consequently α_{spill} depends on the intake design. The inlet lip of supersonic aircraft is usually sharpened to minimize performance losses from shock waves [66] and the cowl thrust is therefore expected to be quite low. In the simulations presented in chapter 4, it was assumed that 10 % of the pre-entry drag could be recovered, i.e. $\alpha_{spill} = 0.9$ was used.

$$D_{spill} = \alpha_{spill} D_{pre} \tag{3.8}$$

$$D_{pre} = (p_c - p_\infty)A_c + \rho_c V_c^2 A_c - \rho_\infty V_\infty^2 A_\infty \tag{3.9}$$

$$C_{D_{pre}} = \frac{D_{pre}}{q_\infty A_c} \tag{3.10}$$

3.3 Engine sizing and design point selection

Experience from previous performed design studies for military jet engines such as [33, 34, 67–70] has formed the basis of the search for a suitable thermodynamic cycle. Several design points have been evaluated during the engine development. The selected design point was found, following an iterative procedure where the engine design point was gradually altered and the impact on the mission design points, simulated as off-design points, was evaluated. Table 3.3 shows some of the key design parameters of the thermodynamic cycle used to produce the simulation results presented in chapter 4.

The chosen design point is balanced to achieve high specific thrust at key parts of the aircraft mission, described in section 2.1 and acceptable SFC for cruise

Table 3.3: Design point characteristics.

Parameter	Value
Altitude	0 m
Mach number	0.0
Fan pressure ratio	5.4
HPC pressure ratio	5.2
Inlet mass flow	90 kg/s
Turbine inlet blade temperature	1030 K
Bypass ratio	0.5
Turbine inlet gas temperature	2000 K
Bleed flow	0 kg/s
LPT power extraction	0 kW
HPT power extraction	0 kW

stages. This was done utilizing experiences from a study presented in [61], where the character of designs with different design OPR was examined, with and without power extraction from the HP shaft. The investigation was performed with a design point $T_4 = 2025$ K and $BPR = 0.4$. Figure 3.2 illustrates the T_4 requirement for different design OPR, to meet the thrust requirement of mission point number 2 of the fighter aircraft mission presented in Table 2.2, the runway acceleration.

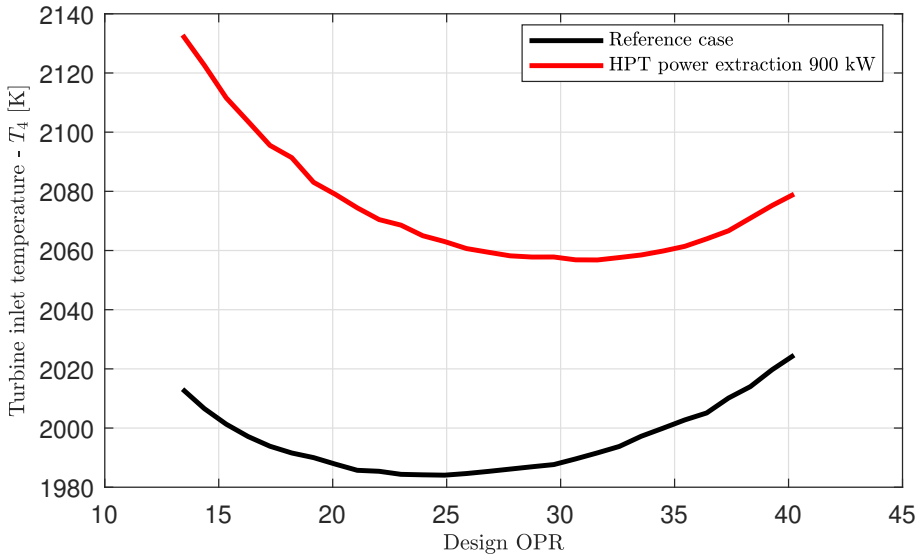

Figure 3.2: Required T_4 for different design OPR, point 2 of the mission thrust requirement, from [61].

A fan pressure ratio (FPR) of 5.4 is hard to achieve with only three fan stages [71]. Adding another fan stage will add extra weight to the fan. Other drawbacks of high FPR is increased specific fuel consumption (SFC) for non-augmented cases (A/B not in operation) and increased temperatures at the later stages of the HPC [8]. Nevertheless, high fan pressure ratio is desirable in fighter jet engines as it increases specific thrust of the engine [1, 8, 72]. This limits the intake cross sectional area and

the aircraft cross-sectional area, which is beneficial for a military aircraft aiming for supersonic flight [7–9, 71]. Moreover, increased specific thrust contributes to reduced engine weight [71], which is also desirable in aircraft designed for military purposes.

The chosen bypass ratio, 0.5 is in the expected range of a modern, low bypass ratio, mixed flow turbofan engine [1, 9, 33, 34, 67, 70].

3.4 Engine constraints and limitations

The solutions to the off design simulations are constrained by maximum turbine inlet temperature T_{4max} and maximum overall pressure ratio OPR_{max}, following a control principle described in [34, 73, 74]. There are of course other limitations to the turbofan engine control, as described in [4, 67, 71, 73], but these limitations are neglected here.

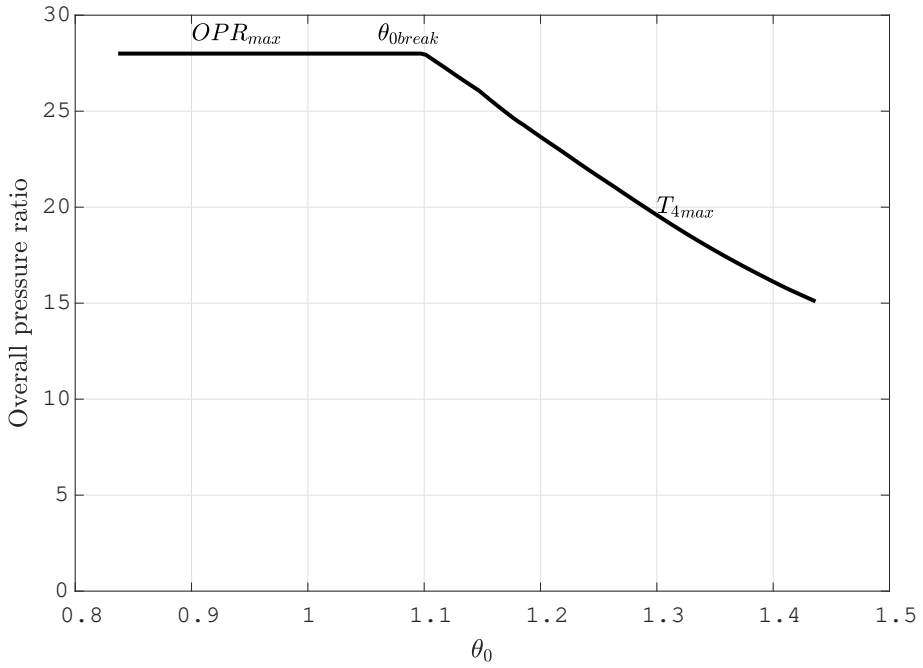

Figure 3.3: Engine control principle, using a method proposed in [34, 73, 74] Overall pressure ratio variation with non-dimensional stagnation temperature θ_0.

The performance of the low bypass ratio mixed flow turbofan engine will be constrained by either OPR_{max} or T_{4max} at military power or maximum augmented power. At low free-stream stagnation temperatures, typically at high altitudes and low speed cases, the engine is limited by OPR_{max} and at high free-stream stagnation temperatures, typically at low altitudes and high speeds, the engine will be constrained by T_{4max} as illustrated in Figure 3.3. The point where the engine switches from OPR_{max} to T_{4max} limitation is referred to as the θ_{0break} [34, 73, 74].

Various combinations of $T_{4_{max}}/OPR_{max}$ have been evaluated throughout the design work. The simulation results presented in chapter 4 are produced with $T_{4_{max}} = 2260K$, the maximum turbine inlet temperature of the F135 jet engine

according to [75] and $OPR_{max} = 28$, balanced to meet the thrust requirements of Table 2.2 in section 2.1 and at the same time limit the required airflow to the engine. Operating the engine at 2260 K, which indeed is a very high temperature, poses challenges with regards to material strengths, thermal corrosion, lifetime of hot parts and cooling requirements [4, 75, 76], but increased turbine inlet temperature improves thermal efficiency and specific thrust of the turbofan engine.

Chapter 4

Simulation results

This chapter summarizes results from off design simulations performed with the low bypass ratio mixed flow turbofan engine described in chapter 3. An evaluation of the specific thrust requirements, presented in section 2.1 is given in section 4.1 and more general predictions on aircraft performance are presented in section 4.2.

4.1 Engine simulations

The simulations have been performed with the following four cases, in terms of power extraction:

1. Baseline - no power extraction (illustrated with black colour)
2. 900 kW HP shaft power extraction (red)
3. 900 kW LP shaft power extraction (blue)
4. Combined shaft power extraction HP shaft 450 kW/LP shaft 450 kW (magenta)

The engine configuration, described in chapter 3 meets the engine thrust requirements of Table 2.2 in section 2.1 for all power extraction cases, with two exceptions, see Figure 4.1.

The LP shaft power extraction case was limited by the OPR_{max} constraint and did not meet the fifth thrust requirement of Table 2.2 and the installed thrust requirement of the tenth thrust requirement was not met by any of the power extraction cases, where the engine is limited by the T_{4max} limitation, as shown in Figure 4.2.

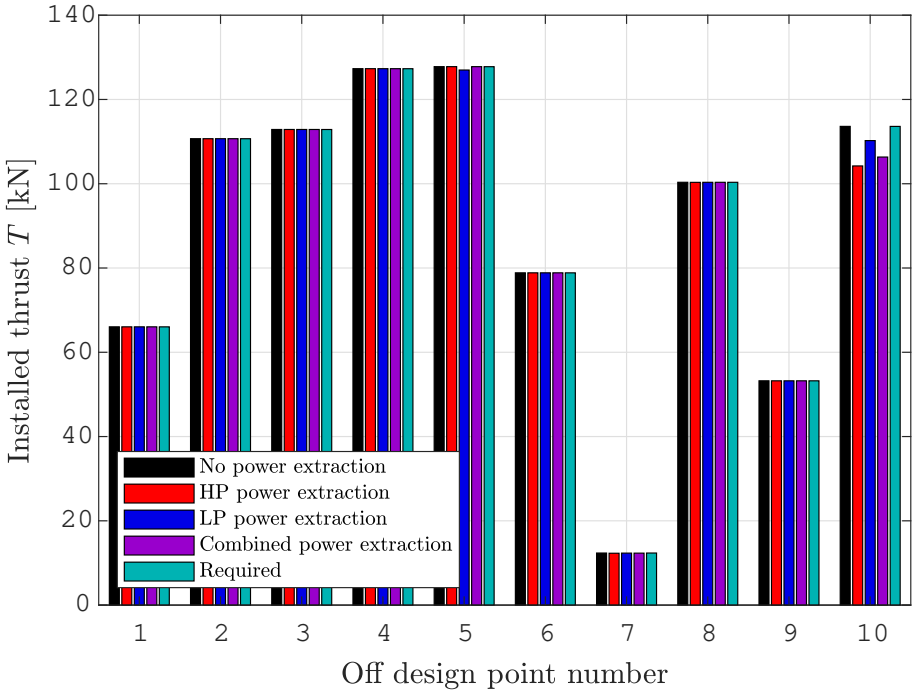

Figure 4.1: Installed thrust versus thrust requirement.

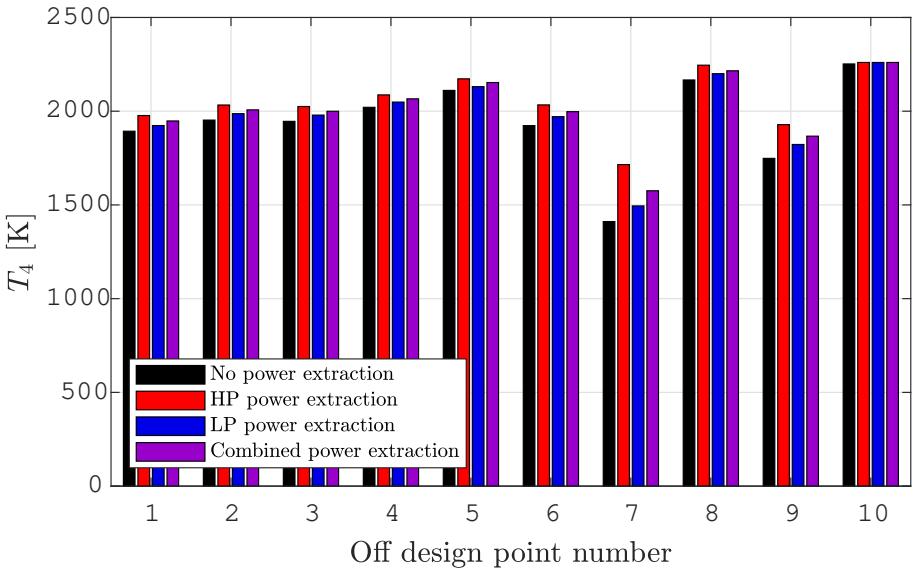

Figure 4.2: Turbine inlet gas temperature.

It can be noted that the HP shaft power extraction case causes the largest thrust reduction in point 10. Figure 4.2 shows that the turbine inlet temperature increase associated with HP shaft power extraction is higher compared to the LP shaft power extraction case. Higher turbine inlet temperature causes increased specific thrust, but also higher specific fuel consumption (SFC) for non-augmented cases, as illustrated by point 1 and 7 in Figure 4.3. Afterburner operation is different in this aspect. In fact, a slight SFC reduction can be achieved if a T_4 increase is acceptable, as illustrated by Figure 4.3. If so, the increased fuel flow of the core engine can be compensated by an afterburner fuel flow reduction.

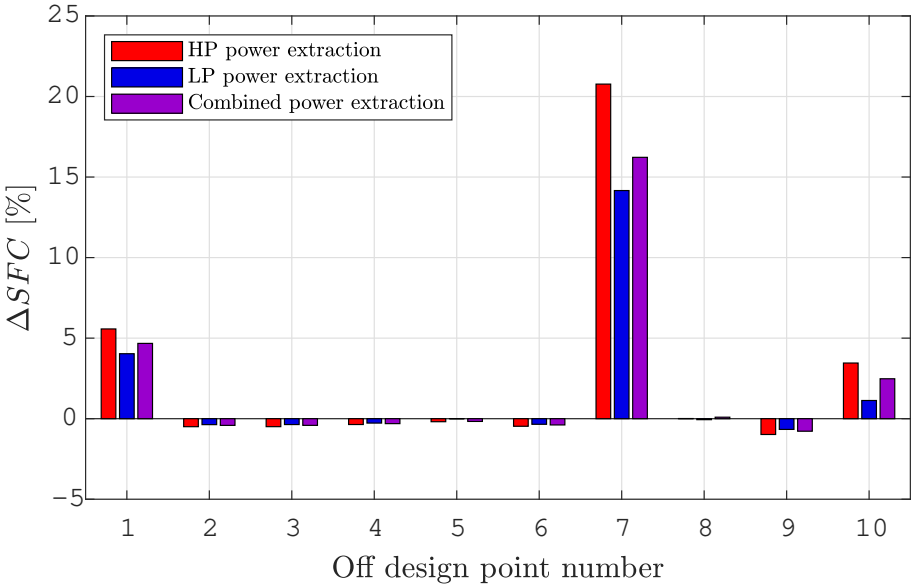

Figure 4.3: Specific fuel consumption relative to Baseline.

Simulations are also performed at military power (MIL, A/B not in operation) and maximum augmented power (MAX, A/B in operation) for various altitudes and Mach numbers. Results from 9 km altitude are presented in Figures 4.4 – 4.11.

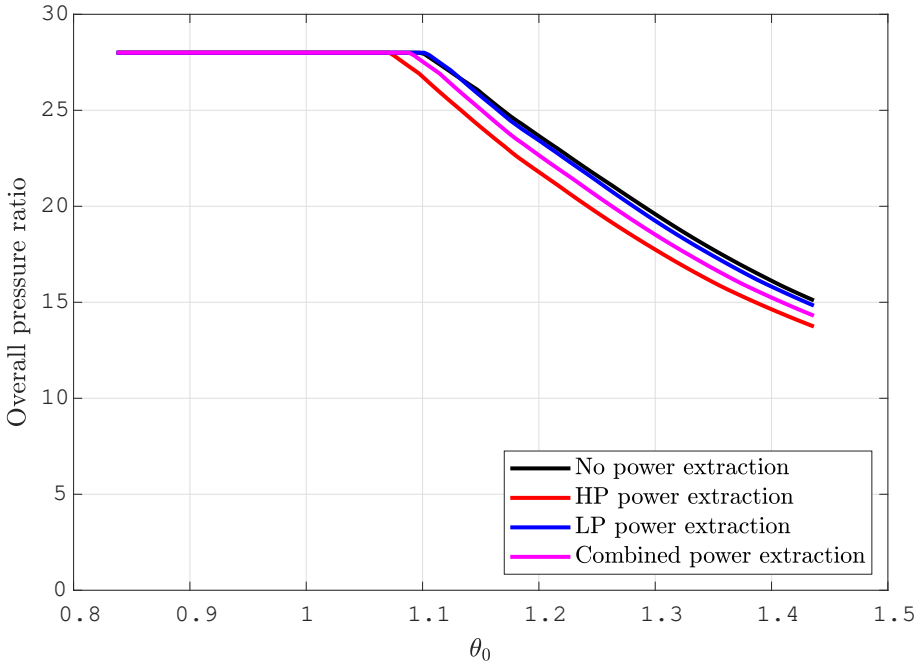

Figure 4.4: OPR versus θ_0, altitude 9 km at military power.

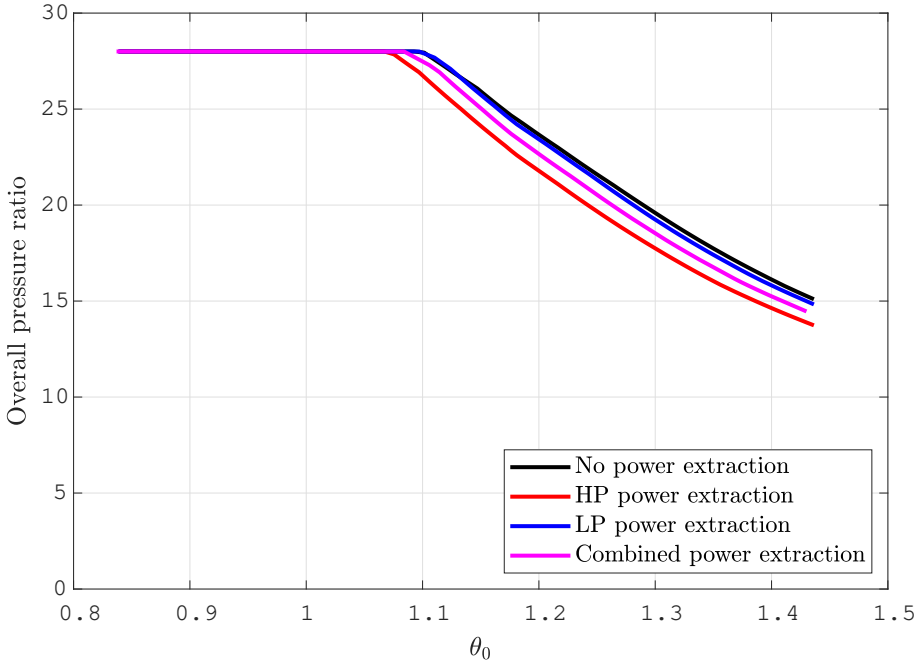

Figure 4.5: OPR versus θ_0, altitude 9 km at MAX power.

Figure 4.4 shows variation of OPR with θ_0 at MIL power. A similar illustration for MAX power is given in Figure 4.5. Figure 4.4 and 4.5 show how the engine is

limited by maximum OPR, OPR_{max} up to the θ_{0break} [34, 73, 74] (located at $\theta_0 = 1.1$ for the baseline case) where the maximum turbine inlet gas temperature, T_{4max} is reached.

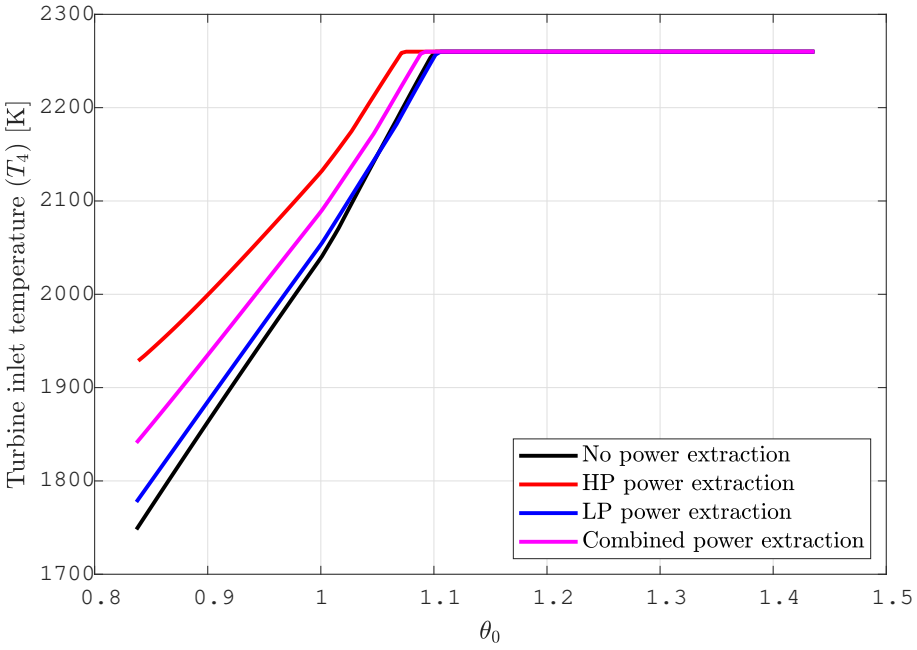

Figure 4.6: T_4 versus θ_0, altitude 9 km at military power.

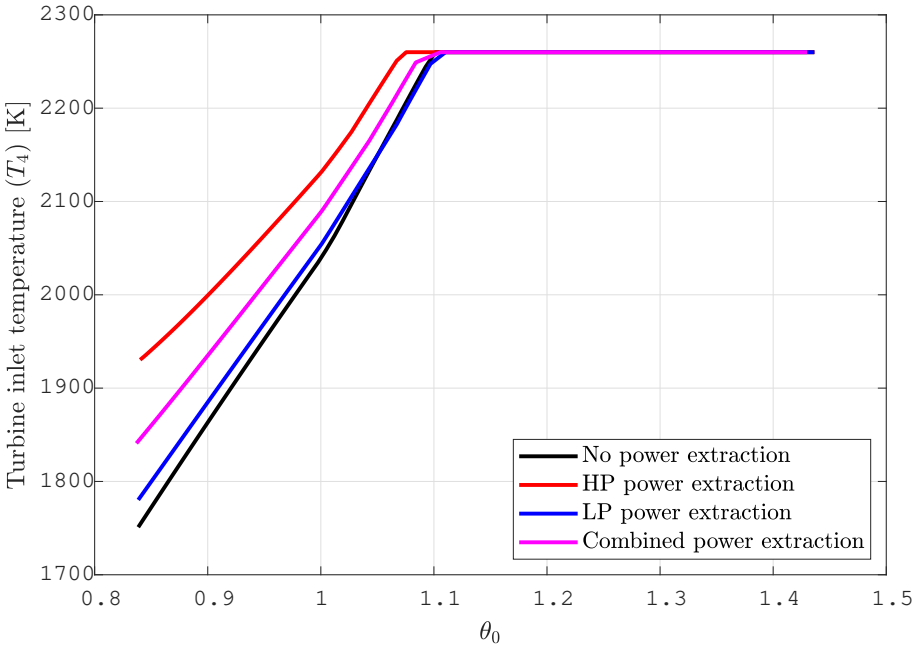

Figure 4.7: T_4 versus θ_0, altitude 9 km at MAX power.

For $\theta_0 > \theta_0$ break, the engine must limit OPR not to exceed the T_{4max} limit. Please note how the θ_{0break} moves to the left when power is extracted from HP shaft. This is due to the temperature increase associated with HP shaft power extraction,

illustrated in Figure 4.6 and Figure 4.7, where turbine inlet temperature T_4 variation with θ_0 is shown for MIL and MAX power respectively. It can be observed that the T_4 deviation between the power extraction cases and the baseline case increases with decreasing θ_0 as the corrected power take-off increases.

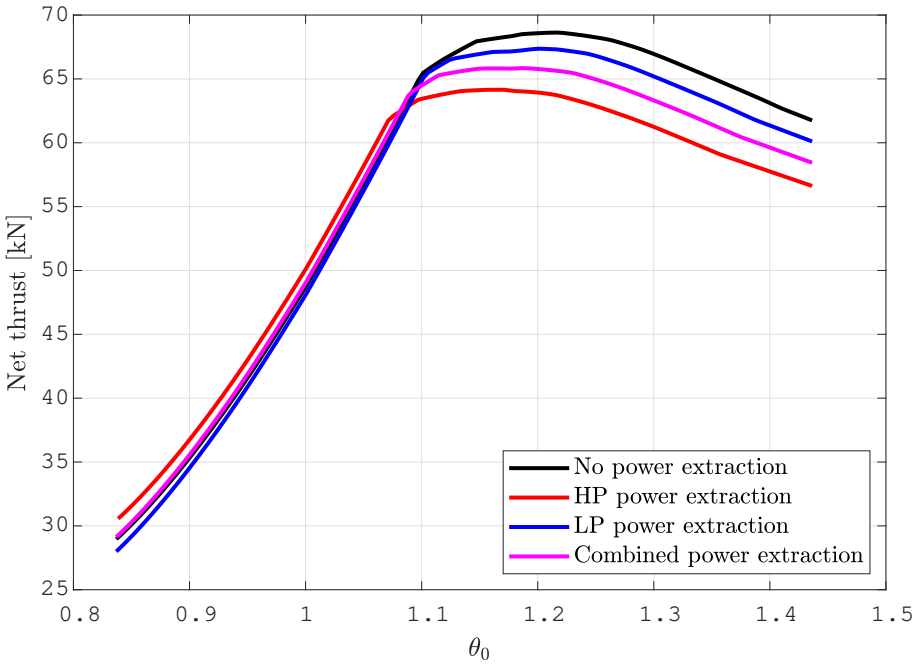

Figure 4.8: Net thrust versus θ_0, altitude 9 km at military power.

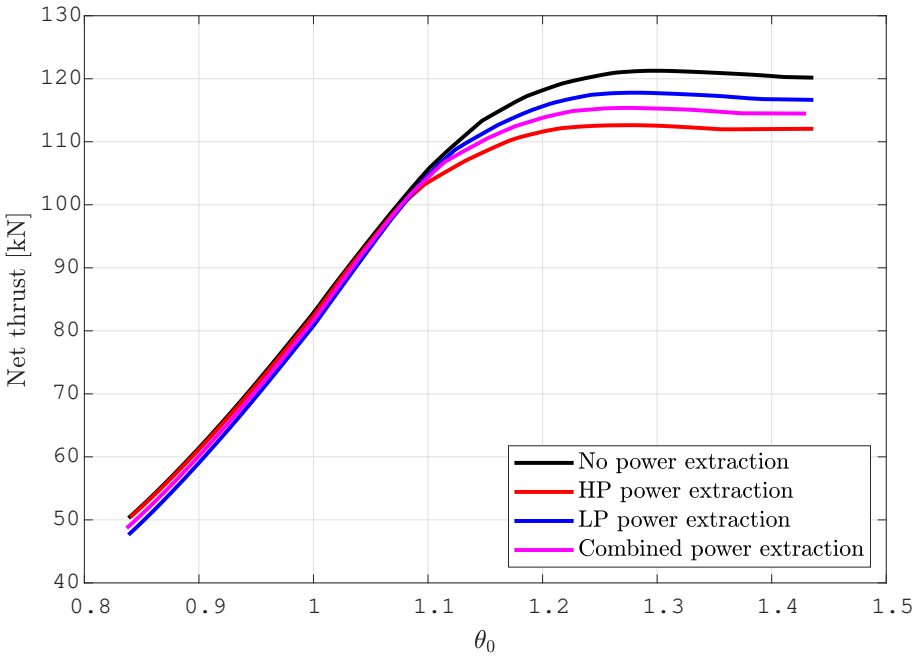

Figure 4.9: Net thrust versus θ_0, altitude 9 km at MAX power.

Engine net thrust, F_N is increased with θ_0 for $\theta_0 < \theta_0$ break, as illustrated by Figure 4.8 and Figure 4.9. When θ_0 exceeds the θ_{0break}, turbine inlet temperature T_4

must be limited to T_{4max} and the net thrust levels out (maximum augmented power) or decreases with increased θ_0 (military power).

Figure 4.10 and Figure 4.11 illustrate SFC variation with θ_0 at MIL and MAX power.

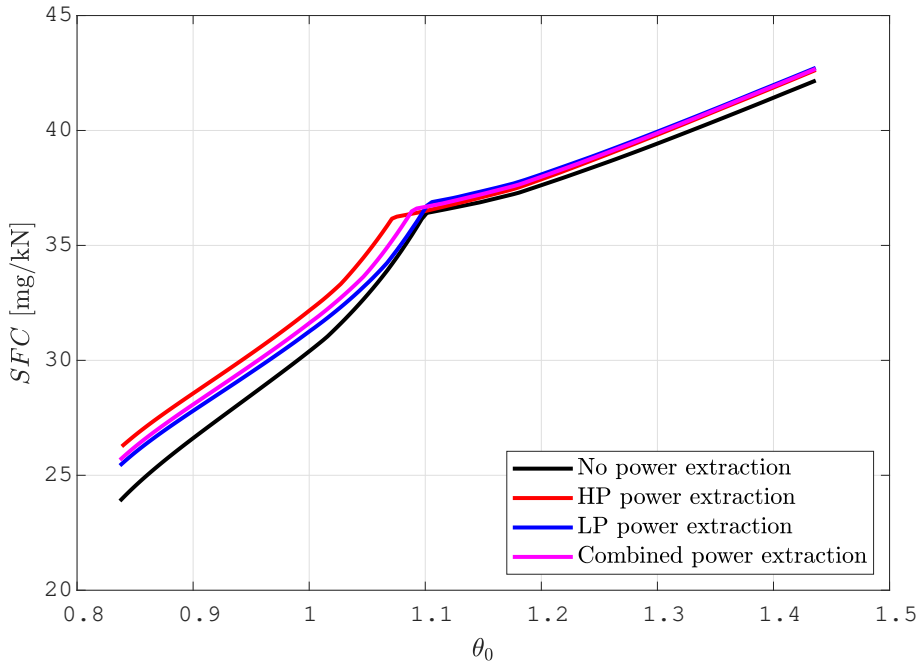

Figure 4.10: SFC versus θ_0, altitude 9 km at military power.

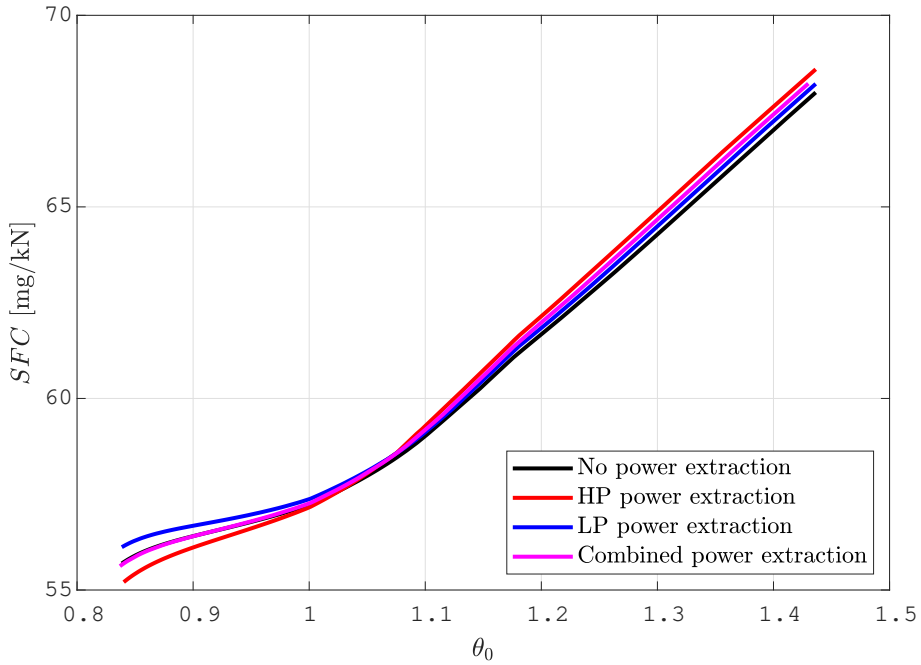

Figure 4.11: SFC versus θ_0, altitude 9 km at MAX power.

As expected, SFC is increased for all θ_0 at military power. As previously observed,

an SFC reduction at maximum augmented power may be achieved for the HP shaft power extraction case if turbine inlet gas temperature is not limited by the T_{4max} limitation. Provided that a sufficient turbine inlet temperature T_4 increase is acceptable, the core fuel flow increase is more than compensated by an A/B fuel flow reduction. This can be explained by the fact that it is always better from a thermal efficiency perspective to add heat at a higher pressure [33], as illustrated by the schematic T-S diagram in Figure 4.12. Figure 4.12 shows the increased core power output with HP shaft power extraction compared to the baseline case.

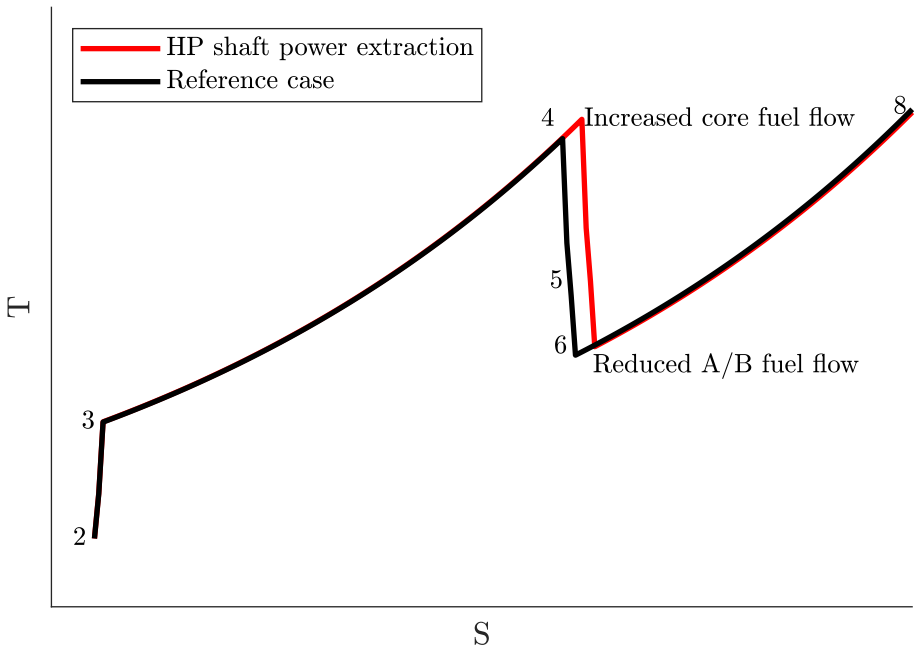

Figure 4.12: Schematic T-S diagram illustrating HP shaft power extraction and no power extraction in maximum augmented operation. The figure is based on Figure 8 in [61].

4.2 Aircraft simulations

Now that the conceptual engine design is carried out as described in chapter 3 and the basic thrust requirements are met, some more general, preliminary predictions on aircraft performance can be made, utilizing the aircraft performance tool described in section 2.2. Performance data produced from a large number of engine performance simulations were used as input to the simulations.

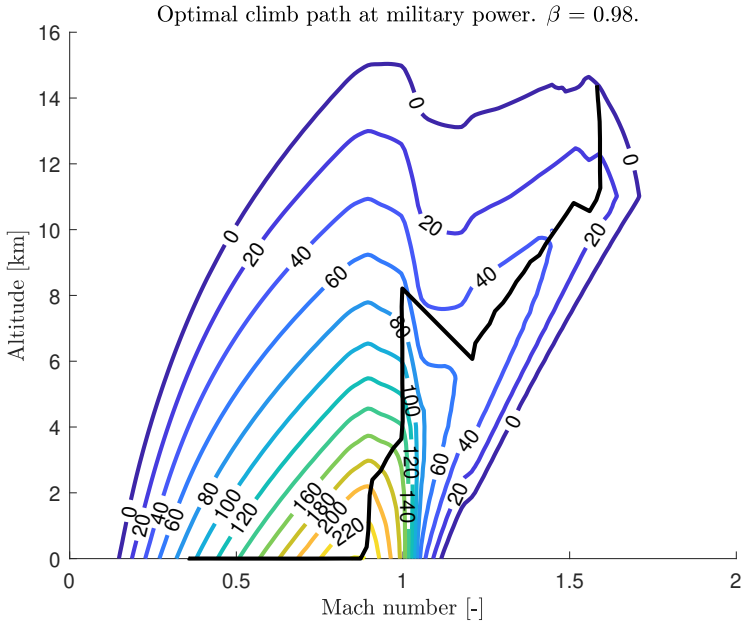

Figure 4.13: P_s and minimum time-to-climb path at military power.

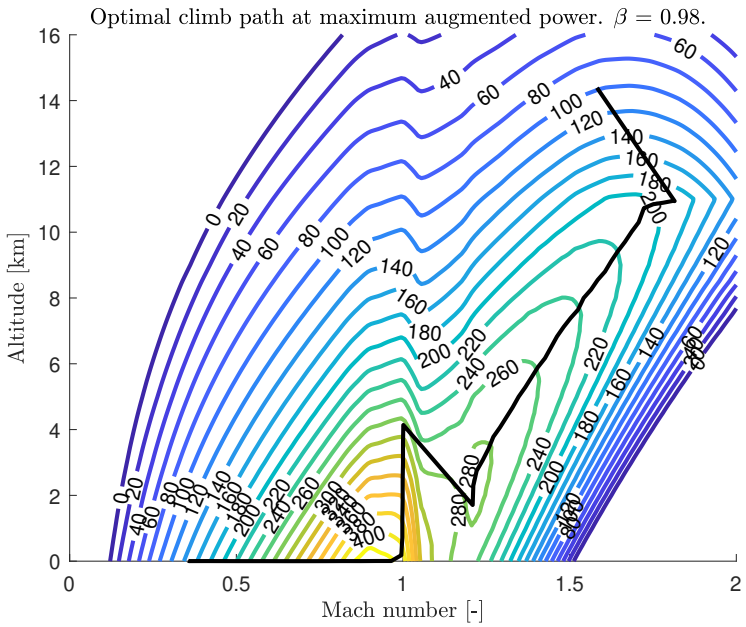

Figure 4.14: P_s and minimum time-to-climb path at maximum augmented power.

Figure 4.13 shows specific excess power, P_s in the flight envelope and the minimum time-to-climb path at military power. The corresponding optimal climb path at maximum augmented power is given in Figure 4.14.

Figure 4.15 illustrates specific range, R_s for typical cruise altitudes and Mach numbers. The maximum specific range at the beginning of the cruise stage, 460 m/kg of fuel were obtained at an optimal altitude of 11.6 km and an optimal Mach number of 0.85. This indicates that the aircraft mission range could be improved if Phase 3 of the mission definition, the cruise stage, is performed at a higher altitude and a somewhat lower Mach number than the specified 9.144 km / M 0.9 of Table 2.2 in section 2.1.

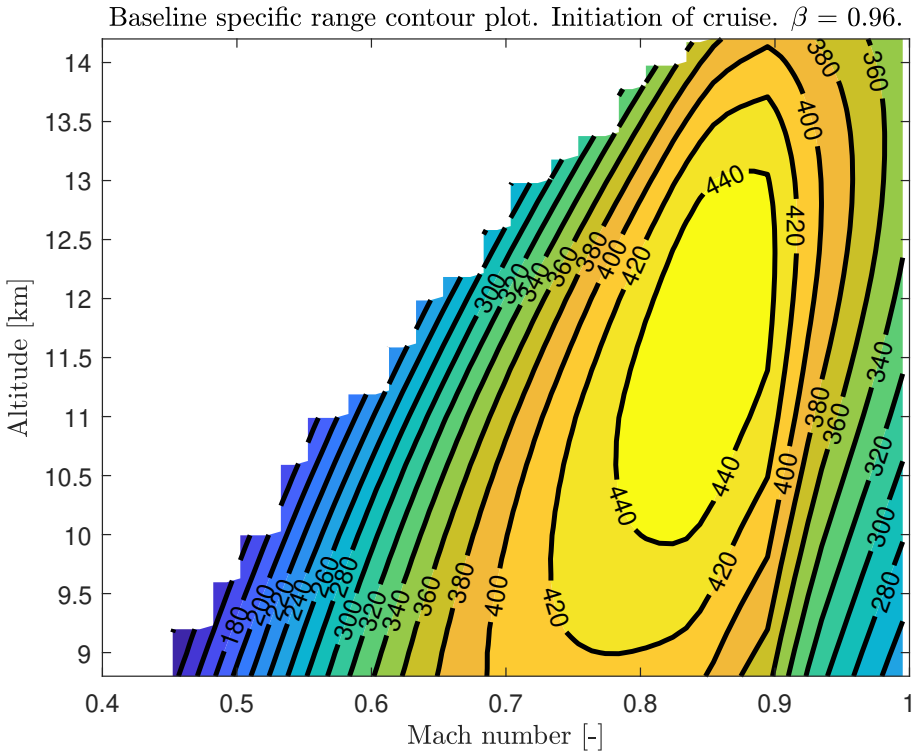

Figure 4.15: Specific range, R_s.

Figure 4.16 illustrates estimated aircraft acceleration at an altitude of 9 km. No specific aircraft acceleration time requirement is specified by University of São Paulo for Phase 6 in the mission definition, but a typical acceleration requirement is given in [43], where a maximum aircraft acceleration time of 50 seconds, for an acceleration from M 0.9 to M 1.5 at 9.144 km altitude is specified. This requirement is illustrated by the dashed blue lines in Figure 4.16. A somewhat harsher requirement is specified in [34] for an acceleration from M 0.8 to M 1.6 within the same acceleration time. This requirement has been slightly reformulated to an acceleration requirement from M 0.9 to M 1.7 within 50 seconds and is visualized by the dashed red lines in Figure 4.16. Figure 4.16 shows that the aircraft acceleration is well below the acceleration requirement, if formulated as in [34, 43]. This indicates that the thrust requirement in point number 10 in Table 2.2, which in practice determines the engine performance in this type of acceleration, is a rather challenging one.

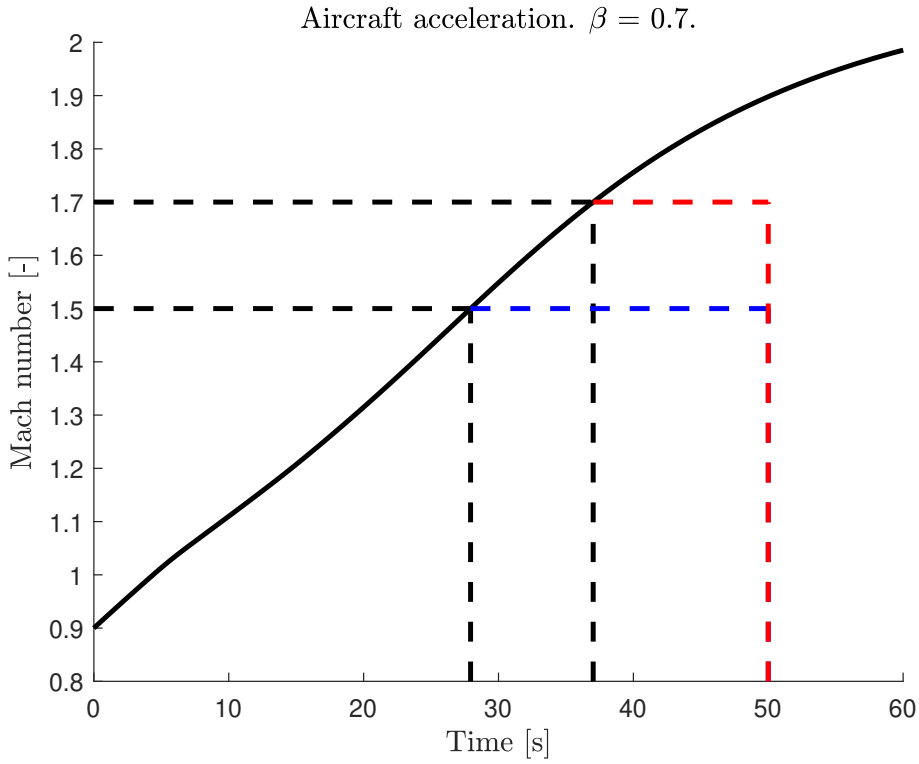

Figure 4.16: Aircraft acceleration.

Chapter 5

Conclusions

A two-spool low bypass ratio mixed flow turbofan engine has been modeled to illustrate the impact of power extraction on engine performance. A thermodynamic engine cycle design has been selected to meet the thrust requirements of the baseline case, i.e. the case where no power is extracted from the jet engine, and a preliminary aircraft / engine interactive performance evaluation has been undertaken to evaluate the cycle design from an aircraft performance perspective. It has been concluded that the two-engine configuration and thermodynamic cycle chosen are well balanced to meet the aircraft performance requirements for the baseline case, while being suitable to illustrate the effects of power extraction.

When power is extracted from the HP or LP shaft of a twin-spool low bypass ratio mixed flow turbofan engine, the turbine inlet temperature is increased. The required temperature increase is higher when power is extracted from the HP shaft. Higher turbine inlet temperatures increases specific thrust and also specific fuel consumption at non-augmented operation. For cases with the afterburner in operation, this turbine inlet temperature increase is favorable as the excess fuel flow of the core engine is compensated by an afterburner fuel flow reduction.

Performance impact of power extraction at military power or maximum augmented power will be highly affected by engine constraints, which in turn are affected by actual flight cases. The solutions of the off-design simulations were constrained by a maximum turbine inlet gas temperature limitation, T_{4max} and a maximum overall pressure ratio limit, OPR_{max}. When the engine is constrained by the OPR_{max} limitation, the increased turbine inlet temperature of the HP shaft power extraction case preserves net thrust more efficiently than the LP shaft power extraction case, provided that the turbine inlet gas temperature increase is acceptable from an engine operability perspective. However, the engine will reach its θ_{0break} for more flight cases when power is extracted from the HP shaft, i.e. the θ_{0break} is reached at lower θ_0 and the performance will be deteriorated for all cases where $\theta_{0break} < \theta_0$. In practice, this means that engine thrust will be reduced considerably at high speed/low altitude cases if power is extracted from the HP shaft. The thrust reduction of the LP shaft power extraction case is more moderate than HP shaft power extraction at these cases. The lower temperature increase of the LP shaft power extraction case allows the engine to operate at higher OPR_{max} for $\theta_{0break} < \theta_0$ compared to the HP shaft

power extraction case.

The research carried out shows that performance benefits can be achieved if power take-off can be distributed between the HP and LP shaft depending on the flight case. However, this might have an impact on the engine design in terms of size and weight. The surge margin of the fan and HPC when no power is extracted might have to be increased to be able to extract power from the HP shaft at $\theta_0 < \theta_{0break}$. An aerodynamic overspeed margin of the HPC is required to maintain thrust of the LP shaft power extraction case for $\theta_0 < \theta_{0break}$. This may have an impact on HPC design, for instance an additional stage could be required.

Bibliography

1. Saravanamuttooo H, Rogers G, Cohen H, Straznicky P, and Nix A. Gas turbine theory. 5th ed. Pearson Education Limited, 2017:101, 127–30, 407–8, 510, 558 (cit. on pp. 3, 21–23).
2. Rolls-Royce plc. The jet engine. 5th ed. The Technical Publication Department. Rolls-Royce plc, 1996:65 (cit. on p. 3).
3. Charrier JJ and Kulshreshtha A. Electric actuation for flight and engine control; evolution and current trend. In: *45th AIAA Aerospace Sciences Meeting and Exhibit*. 2007:1391 (cit. on pp. 3, 4).
4. Langton R and MacIsaac B. Gas turbine propulsion systems. John Wiley & Sons, 2011:63–5, 184–6 (cit. on pp. 3, 23, 24).
5. Demel HF. Installation of electric generators on turbine engines. NASA. Lewis Research Center Aircraft Elect. Secondary Power 1983 (cit. on p. 3).
6. Richter E and Neumann T. Jet Engine Integrated Generator. Journal of Energy 1982;6:45–8 (cit. on pp. 3, 7).
7. Mattingly JD, Boyer KM, and Ohain H von. Elements of propulsion: gas turbines and rockets. American Institute of Aeronautics and Astronautics Reston, VA, 2006:27 (cit. on pp. 3, 23).
8. Lewis G. The next European engine for combat aircraft. The Aeronautical Journal 1984;88:1–9 (cit. on pp. 3, 22, 23).
9. Kurzke J. The mission defines the cycle: turbojet, turbofan and variable cycle engines for high speed propulsion. Tech. rep. NATO Research and Technology Organisation, RTO-EN-AVT-185-02, Dachau, Germany, 2010 (cit. on pp. 3, 7, 23).
10. Palmberg S and Westroth S. Model-based concept development of system in UAV. 2020 (cit. on pp. 3, 4).
11. Drego A and Steinkellner S. A system integrator's perspective on vehicle system evaluation at the aircraft concept stage. 2022 (cit. on pp. 3, 4).
12. Raymond E. Secondary Power System Options for Future Military Aircraft. SAE Transactions 1980:3593–612 (cit. on p. 4).
13. Mahefkey T, Yerkes K, Donovan B, and Ramalingam M. Thermal management challenges for future military aircraft power systems. Journal of Aerospace 2004;113:1965–73 (cit. on p. 4).

14. Walters E, Amrhein M, O'Connell T, Iden S, Lamm P, Yerkes K, Wolff M, McCarthy K, Raczkowski B, Wells J, et al. INVENT modeling, simulation, analysis and optimization. In: *48th AIAA Aerospace Sciences Meeting Including the New Horizons Forum and Aerospace Exposition*. 2010:3 (cit. on p. 4).

15. Clark R, Shi M, Gladin J, and Mavris D. Design and analysis of an aircraft thermal management system linked to a low bypass ratio turbofan engine. J. Eng. Gas Turbines Power 2022;144 (cit. on p. 4).

16. Oyori H, Morioka N, Kakiuchi D, Shimomura Y, Onishi K, and Sano F. System design for the more electric engine incorporated in the electrical power management for more electric aircraft. Tech. rep. SAE Technical Paper, 2012 (cit. on p. 4).

17. Boglietti A, Cavagnino A, Tenconi A, and Vaschetto S. The safety critical electric machines and drives in the more electric aircraft: A survey. In: *2009 35th Annual Conference of IEEE Industrial Electronics*. IEEE. 2009:2587–94 (cit. on p. 4).

18. Rosero J, Ortega J, Aldabas E, and Romeral L. Moving towards a more electric aircraft. IEEE Aerospace and Electronic Systems Magazine 2007;22:3–9 (cit. on p. 4).

19. Eek M. On credibility assessment in aircraft system simulation. PhD thesis. Linköping University Electronic Press, 2016 (cit. on pp. 4, 5).

20. Cloyd JS. A status of the United States Air Force's more electric aircraft initiative. In: *IECEC-97 Proceedings of the Thirty-Second Intersociety Energy Conversion Engineering Conference (Cat. No. 97CH6203)*. Vol. 1. IEEE. 1997:681–6 (cit. on p. 4).

21. Quigley R. More electric aircraft. In: *Proceedings Eighth Annual Applied Power Electronics Conference and Exposition,* IEEE. 1993:906–11 (cit. on p. 4).

22. Heerden AS van, Judt DM, Jafari S, Lawson CP, Nikolaidis T, and Bosak D. Aircraft thermal management: Practices, technology, system architectures, future challenges, and opportunities. Progress in Aerospace Sciences 2022;128:100767 (cit. on pp. 4, 5).

23. Doman DB. Rapid mission planning for aircraft thermal management. In: *AIAA guidance, navigation, and control conference*. 2015:1076 (cit. on p. 4).

24. Freeman J, Osterkamp P, Green M, Gibson A, and Schiltgen B. Challenges and opportunities for electric aircraft thermal management. Aircraft Engineering and Aerospace Technology: An International Journal 2014 (cit. on p. 4).

25. Chapman JW. A Study of Large Scale Power Extraction and Insertion on Turbofan Performance and Stability. In: *2020 AIAA/IEEE Electric Aircraft Technologies Symposium (EATS)*. IEEE. 2020:1–17 (cit. on pp. 4, 5).

26. Zähringer C, Stastny K, and Ardey S. Towards the powerhouse for more electric aircraft–dedicated engine concepts. In: *Proceedings of the 19th International Symposium on Air Breathing Engines*. 2009 (cit. on pp. 4, 5).

27. Pluijms A, Schmidt KJ, Stastny K, and Chibisov B. Performance comparison of more electric engine configurations. In: *Turbo Expo: Power for Land, Sea, and Air*. Vol. 43116. 2008:113–22 (cit. on pp. 4, 5, 7).

28. Culley DE, Kratz JL, and Thomas GL. Turbine Electrified Energy Management (TEEM) for enabling more efficient engine designs. In: *2018 Joint Propulsion Conference, Cincinnati, OH, USA*. 2018:4798 (cit. on pp. 4, 5).

29. Faidi A. Effect of Accessory Power Take-Off Variation on a Turbofan Engine Performance. Wright- Patterson Air Force Bace: Dayton, OH, USA, 2012 (cit. on p. 4).

30. Corbett M. Shaft power extraction and waste heat rejection using a three stream variable cycle engine. SAE International Journal of Aerospace 2012;5:371 (cit. on pp. 4, 7).

31. Meng X, Yang X, Chen M, and Zhu Z. High-level power extraction from adaptive cycle engine for directed energy weapon. In: *2018 Joint Propulsion Conference*. 2018:4518 (cit. on p. 4).

32. Grönstedt T. Development of methods for analysis and optimization of complex jet engine systems. Chalmers Tekniska Högskola (Sweden), 2000 (cit. on pp. 6, 17, 18).

33. Kurzke J and Halliwell I. Propulsion and power: an exploration of gas turbine performance modeling. Springer, 2018:12, 33, 34, 49, 97, 99 (cit. on pp. 7, 21, 23, 32).

34. Mattingly JD. Aircraft engine design. Aiaa, 2002:16, 17, 112, 123, 172, 341, 462, 465, 478, 525–6 (cit. on pp. 7, 9, 10, 20, 21, 23, 29, 35).

35. Mastropierro FS, Sebastiampillai J, Jacob F, and Rolt A. Modeling Geared Turbofan and Open Rotor Engine Performance for Year-2050 Long-Range and Short-Range Aircraft. Journal of Engineering for Gas Turbines and Power 2020;142 (cit. on p. 7).

36. Rosell D, Grönstedt T, Bravo-Mosquera PD, and Martini Catalano F. Low BPR turbofan performance with power extraction. In: *33rd Congress of the International Council of the Aeronautical Sciences, Stockholm*. 2022 (cit. on pp. 9–11, 19).

37. Sacher P, Orlik-Rückmann K, Gödel H, Costes B, Leynaert J, Perrier P, Bore C, Sellars R, Lamar J, Parker J, et al. Special course on fundamentals of fighter aircraft design. AGARD Report 1986;740 (cit. on p. 9).

38. Ball RE. The fundamentals of aircraft combat survivability: analysis and design. American Institute of Aeronautics and Astronautics, 2003 (cit. on p. 9).

39. Endsley MR. A survey of situation awareness requirements in air-to-air combat fighters. The International Journal of Aviation Psychology 1993;3:157–68 (cit. on p. 9).

40. Mavris D and DeLaurentis D. An integrated approach to military aircraft selection and concept evaluation. In: *Aircraft Engineering, Technology, and Operations Congress*. 1995:3921 (cit. on p. 9).

41. Bennett Jr W, Schreiber BT, and Andrews DH. Developing competency-based methods for near-real-time air combat problem solving assessment. Computers in Human Behavior 2002;18:773–82 (cit. on p. 9).

42. Bravo-Mosquera PD, Abdalla AM, Cerón-Muñoz HD, and Catalano FM. Integration assessment of conceptual design and intake aerodynamics of a non-conventional air-to-ground fighter aircraft. Aerospace Science and Technology 2019;86:497–519 (cit. on pp. 10, 15, 20).

43. Raymer D. Aircraft Design: A Conceptual Approach. American Institute of Aeronautics and Astronautics, Inc., 2018:36, 396, 436–9, 637, 639, 643, 662, 664, 667, 719 (cit. on pp. 12–15, 35).

44. Anderson JD. Aircraft performance and design. Vol. 1. WCB/McGraw-Hill Boston, 1999:293, 310, 314, 345, 348, 351 (cit. on pp. 12, 13).

45. Nicolai LM and Carichner GE. Fundamentals of aircraft and airship design, Volume 1–Aircraft Design. American Institute of Aeronautics and Astronautics, 2010 (cit. on pp. 12–15).

46. Karlsson A. Take-off and landing performance. SA105X-Flygteknik vt2013 2010 (cit. on p. 12).

47. Covert E. Thrust and drag: Its prediction and verification. AIAA Progress in Astronautics and Aeronautics 1985;98:131–3, 145–6, 151–3 (cit. on pp. 14, 15).

48. Jobe CE. Prediction and verification of aerodynamic drag, part I: prediction. Progress in Astronautics and Aeronautics, edited by CE Eugene 1985;98 (cit. on pp. 14, 15).

49. Sears WR. On projectiles of minimum wave drag. Quarterly of Applied Mathematics 1947;4:361–6 (cit. on p. 14).

50. Schemensky RT. Development of an Empirically Based Computer Program to Predict the Aerodynamic Characteristics of Aircraft. Volume II. Program User Guide. Tech. rep. General Dynamics Corporation, Convair Aerospace Division, Fort Worth, Texas, 1973 (cit. on p. 15).

51. Saravanamuttoo H. The mission defines the cycle: turbojet, turbofan and variable cycle engines for high speed propulsion. Tech. rep.:1.1–1.18 (cit. on p. 17).

52. Benner P, Bollhöfer M, Kressner D, Mehl C, and Stykel T. Numerical algebra, matrix theory, differential-algebraic equations and control theory. Springer, 2015:ix, 463 (cit. on p. 18).

53. Campbell SL, Linh VH, and Petzold LR. Differential-algebraic equations. Scholarpedia 2008;3:2849 (cit. on p. 18).

54. Ascher UM and Petzold LR. Computer methods for ordinary differential equations and differential-algebraic equations. Vol. 61. Siam, 1998:12 (cit. on p. 18).

55. Grönstedt T. Advanced solvers for general high performance transient gas turbine simulation tools. In: *14th International Symposium on Air Breathing Engines, Florence, Italy*. 1999 (cit. on p. 18).

56. Petzold LR. Numerical methods for differential-algebraic equations: Current status and future directions. 1989 (cit. on p. 18).

57. Campbell S, Ilchmann A, Mehrmann V, Reis T, et al. Applications of differential-algebraic equations: examples and benchmarks. Springer, 2019 (cit. on p. 18).

58. Broyden CG. A class of methods for solving nonlinear simultaneous equations. Mathematics of computation 1965;19:577–93 (cit. on p. 18).

59. Broyden C. A new method of solving nonlinear simultaneous equations. The Computer Journal 1969;12:94–9 (cit. on p. 18).

60. Press WH, Vetterling WT, Teukolsky SA, and Flannery BP. Numerical Recipes in FORTRAN: The Art of Scientific Computing. Cambridge University Press Cambridge UK, 1992 (cit. on p. 18).

61. Rosell D and Grönstedt T. Design Considerations of Low Bypass Ratio Mixed Flow Turbofan Engines with Large Power Extraction. Fluids 2022;7:21 (cit. on pp. 19, 22, 32).

62. ARP755B S. Aircraft Propulsion System Performance Station Designation and Nomenclature. SAE ARP755 Rev. B 1994 (cit. on p. 18).

63. Stenfelt M. On model based aero engine diagnostics. PhD thesis. Mälardalens universitet, 2023:30 (cit. on p. 20).

64. Seddon J and Goldsmith EL. Intake aerodynamics. Vol. 1. Collins Professional and Technical Books, 1985:219–20 (cit. on pp. 20, 21).

65. Yuhas A and Ray R. Effects of bleed air extraction of thrust levels on the F404-GE-400 turbofan engine. In: *28th Joint Propulsion Conference and Exhibit*. 1992:3092 (cit. on p. 20).

66. El-Sayed AF and Emeara MS. Intake of aero-engines: a case study. In: *The International conference of engineering sciences & applications*. 2016 (cit. on p. 21).

67. Grieb H. Projektierung von turboflugtriebverken. Springer: Basel, Switzerland, 2004:562–4, 735 (cit. on pp. 21, 23).

68. Nadon LJ, Kramer SC, and King PI. Multidisciplinary optimization in conceptual design of mixed-stream turbofan engines. Journal of propulsion and power 1999;15:17–22 (cit. on p. 21).

69. Mattingly J and Heiser W. Performance estimation of the mixed flow, afterburning, cooled, two-spool turbofan engine with bleed and power extraction. In: *22nd Joint Propulsion Conference*. 1986:1757 (cit. on p. 21).

70. Mattingly J. Performance estimation of some variable bypass ratio turbofan engines. In: *34th AIAA/ASME/SAE/ASEE Joint Propulsion Conference and Exhibit*. 1998:3894 (cit. on pp. 21, 23).

71. Olsson U. Aerospace propulsion from insects to spaceflight. 2006:186, 289, 297, 395, 412, 416, 432, 434, 479, 505 (cit. on pp. 22, 23).

72. Guha A. Optimum fan pressure ratio for bypass engines with separate or mixed exhaust streams. Journal of Propulsion and Power 2001;17:1117–22 (cit. on p. 22).

73. Jaw L and Mattingly J. Aircraft engine controls. American Institute of Aeronautics and Astronautics New York, NY, USA, 2009 (cit. on pp. 23, 29).

74. Mattingly J. Easy method of matching fighter engine to airframe for use in aircraft engine design courses. In: *25th Joint Propulsion Conference*. 1989:2260 (cit. on pp. 23, 29).

75. Langston LS. Fahrenheit 3,600. mechanical engineering 2007;129:34–7 (cit. on p. 24).

76. Oates GC. Aircraft propulsion systems technology and design. Aiaa, 1989:7, 8, 50, 64 (cit. on p. 24).